

# Heat storage in lead-acid accumulators on-board submarines

Henrik Hed

*Thesis for the Degree of Master of Science*

---

Division of Fluid Mechanics  
Department of Energy Sciences  
Faculty of Engineering, LTH  
Lund University  
P.O. Box 118  
SE-221 00 Lund  
Sweden



© Henrik Hed

ISRN LUTMDN/TMHP 11/5235-SE

ISSN 0282-1990

Printed in Sweden

Lund 2011

## Abstract

A Swedish submarine often operates in colder waters, resulting in a cold on-board climate and a low temperature in the batteries. The batteries reach their maximum capacity when they are at a temperature of 30°C, which they rarely are during the winter months when the temperature often is lower than 7°C. The diesel engines are producing a significant amount of waste heat that is just dispersed into the sea. By using this waste heat and storing it in the batteries would the capacity of the batteries be better and the on-board climate as well. The heat transfer to the battery cell will be through an existing cooling system in the pole bridge together with internal heat generation from different charging levels. This cooling system has a limited reach into the cell making the ability to spread heat inside the cell limited. The main question to investigate is how well this heat will distribute and how much energy that can be stored over time inside a battery cell.

The primary method has been to create a realistic CAD model of a battery cell that later on has been used for simulation through a CFD analysis. To create a realistic model previous calculations and schematics have been studied and interviews with the supplier of the cell and Kockums AB employees have been performed. Furthermore, analytical calculations for both simplifications of the geometry and the potential of proposed method have been done.

The available waste heat from the diesel engines through the cooling water is about 2,7MW, which is more than needed since the pole bridge has a maximum delivered heat of 912W/bridge. The heat storage potential is 18,8 MJ per double cell and all the cells together form an energy storage with far greater capacity than a regular accumulator tank in for example a villa. This is estimated to be enough to make the on-board climate more pleasant. This is also confirmed by previous crew members who points out that when the batteries are warm, the climate on-board is also better.

The results showed that the heating from the pole bridge was faster than expected. Already after 20 % of the time of heating combined with stage 1 charge the energy storage had reached 30 % of the full potential. After full time this factor had reached 67 % which corresponds to 12,6 MJ stored heat per double cell. The local temperatures inside the cell during the first case varies significantly and reaches its highest value after 40 % of full time when the temperature difference between the top electrolyte and the electrolyte pumped from the bottom is over 20°C. The trend after full time is that the average temperature is flattened out, which suggests that the cell already is near its steady state.

Heating and stage 2 charging starts at the values reached after stage 1 charge and since the trend of the temperature rise already was flattened out the temperatures during case 2 are not increasing by so much. The average temperature is only increased by less than 5°C and the energy stored after stage 2 charge is just slightly increased to 72 % of full capacity.

The conclusion is that it is possible to store heat in the batteries but further work has to be done. The potential heat storage and available heat has been confirmed to be large enough, the heat transfer from the pole bridge is bigger than expected resulting in a quicker heating of the cell. However, big differences of local temperatures inside the cell were observed, which may result in stratifications that will affect the chemical process when charging. Further work also needs to be done to determine how much of the stored heat is radiated directly out to the sea and for how long the heat source will affect the climate on-board the submarine.

## **Acknowledgements**

I would first and foremost like to thank Magnus Fast who has been my supervisor during my diploma work at Kockums AB. Thanks for the guidance, support, the interest taken in the project and all the help with the report.

My supervisor at LTH, Johan Revstedt has been giving a great support during hard times and always with positive attitude discussed my problems. Thank you.

I would also like to thank Tor Göransson and Henrik Gustafsson for the contribution of your extensive knowledge and your helpfulness.

Thanks to everybody at the department of mechanical engineering at Kockums AB for making me feel welcome and helping me with whatever problem I was handling. Special thanks to Hans Jönsson for the opportunity to perform my diploma work in his group at Kockums AB.

# Table of contents

<b>TABLE OF CONTENTS</b> .....	<b>5</b>
<b>NOMENCLATURE</b> .....	<b>7</b>
<b>ABBREVIATIONS</b> .....	<b>7</b>
<b>1 INTRODUCTION</b> .....	<b>8</b>
1.1 BACKGROUND .....	8
1.2 OBJECTIVES .....	9
1.3 LIMITATIONS .....	9
1.4 METHODS .....	10
1.5 OUTLINE OF THE THESIS.....	10
<b>2 SUBMARINE PROPULSION</b> .....	<b>11</b>
2.1 THE DIESEL ENGINES.....	11
2.2 THE STIRLING ENGINES.....	11
2.3 PROPULSION BY BATTERIES .....	12
2.3.1 <i>The battery cell</i> .....	12
2.3.2 <i>Charging</i> .....	13
<b>3 NUMERICAL METHOD AND TURBULENCE MODELING</b> .....	<b>14</b>
3.1 NUMERICAL SOLVER .....	14
3.2 DISCRETIZATION METHOD .....	14
3.2.1 <i>Energy equation</i> .....	16
3.3 THE MODEL OF TURBULENCE .....	17
3.3.1 <i>K-ε realizable model</i> .....	17
3.4 THE SIMPLE ALGORITHM.....	18
<b>4 AVAILABLE WASTE HEAT AND POTENTIAL HEAT STORAGE CAPACITY</b> .....	<b>19</b>
4.1 WASTE HEAT FROM THE DIESEL ENGINES.....	19
4.1.1 <i>Exhaust gases</i> .....	19
4.1.2 <i>Cooling water</i> .....	20
4.2 POTENTIAL HEAT STORAGE IN THE BATTERIES .....	21
4.3 POTENTIAL TRANSFER OF HEAT FROM THE POLE BRIDGE .....	22
<b>5 GEOMETRY AND MESH GENERATION</b> .....	<b>23</b>
5.1 PROGRAM .....	23
5.2 GEOMETRY .....	23
5.2.1 <i>Geometry generation</i> .....	23
5.3 SIMPLIFICATION OF THE GEOMETRY .....	25
5.3.1 <i>Plate packages</i> .....	25
5.3.1.1 Acid outside the plate package .....	25
5.3.1.2 Calculating the average specific heat .....	26
5.3.1.3 Calculating the average density .....	26
5.3.1.4 Calculating the total thermal conductivity.....	27
5.3.2 <i>Lower pole bridges</i> .....	30
5.3.3 <i>Vertical plates connecting the pole bridges</i> .....	31
5.4 MESH GENERATION.....	32
5.4.1 <i>The meshing method</i> .....	32

<b>6</b>	<b>SIMULATION OF HEAT ABSORPTION IN A BATTERY CELL</b>	<b>34</b>
6.1	GENERAL CONDITIONS	34
6.1.1	<i>Computational settings</i>	34
6.1.2	<i>Monitor points and contour planes</i>	35
6.2	FICTIVE MISSION TO SIMULATE	37
6.3	THE INTERNAL HEAT GENERATION	38
6.4	CASE 1: HEATING COMBINED WITH STAGE 1 CHARGING	40
6.4.1	<i>Conditions</i>	40
6.4.2	<i>Results and comments</i>	40
6.4.2.1	Contours after 3,3 % of full time	42
6.4.2.2	Contours after 10 % of full time	43
6.4.2.3	Contours after 30 % of full time	44
6.4.2.4	Contours after 60 % of full time	45
6.4.2.5	Contours after full time	46
6.5	CASE 2: HEATING COMBINED WITH STAGE 2 CHARGING	47
6.5.1	<i>Conditions</i>	47
6.5.2	<i>Results and comments</i>	47
6.5.2.1	Contours after full time of stage 2 charge	49
<b>7</b>	<b>DISCUSSION AND CONCLUSIONS</b>	<b>50</b>
<b>8</b>	<b>FUTURE WORK</b>	<b>51</b>
	<b>REFERENCES</b>	<b>52</b>
	<b>APPENDIX A: COMPLETE CALCULATIONS</b>	<b>53</b>

# Nomenclature

Greek characters	Declaration	Unit
$\delta$	Thickness	[m]
$\Delta$	Difference	[-]
$\eta$	Efficiency	[-]
$\lambda$	Thermal conductivity	[W/(mK)]
$\mu$	Fraction	[-]
$\rho$	Density	[kg/m <sup>3</sup> ]

Latin letters	Declaration	Unit
A	Area	[m <sup>2</sup> ]
b	Length/width	[m]
$c_p$	Specific heat	[kJ/kg °C]
dQ	Heat generation	[Ws]
h	Enthalpy	[kJ/kg]
I	Current	[A]
L	Length	[m]
m	Mass	[kg]
$\dot{m}$	Mass flow	[kg/s]
N	Amount	[-]
P	Power/heat	[W]
Q	Energy	[J]
R	Resistance (help unit)	[K/W]
t	Time	[h]
T	Temperature	[°C]
u	Help unit	[m]
U	Voltage	[V]
V	Volume	[m <sup>3</sup> ]
$\dot{V}$	Volume flow	[m <sup>3</sup> /s]

# Abbreviations

CAD	Computer Aided Design
CFD	Computational Fluid Dynamics
FMV	Swedish Defence Materiel Administration
GTD	Gotland
AIP	Air Independent Propulsion
AFR	Air-Fuel Ratio
Pb	Lead
Cu	Copper
avg	Average

# 1 Introduction

## 1.1 Background

The main objective for a submarine is to be able to stay under water long enough for their mission to be executed without being detected by leaving signatures. When a submarine is submerged the biggest problem is the absence of atmospheric air that most combustion engines are dependent of. Some submarine manufacturers have solved this problem by using nuclear power for propulsion, but Kockums AB have chosen a different path. They use diesel engines when atmospheric air is accessible and batteries or Stirling engines in submerged mode.

The Stirling engines are a part of the energy system called air independent propulsion (AIP) and use oxygen instead of atmospheric air for the combustion process. Oxygen in liquefied form occupies relatively little space and makes it possible to use a combustion engine for propulsion in submerged mode. To reach a higher speed or sneak with low signatures it is possible to use the batteries for propulsion, but they are limited to a relatively short utilization time before they need to be recharged by the diesel engines.

Swedish submarines often operate in northern Europe where the seawater usually is very cold, especially during the winter months, resulting in the unwanted effect of a low temperature on-board and a reduction of the battery capacity. Even when the submarines are to berth, it is cold on-board due to the lack of open space making it inefficient to use fan heaters for temperature control.

A submarine's diesel engines are used for producing electricity for propulsion and battery recharging but are also producing significant amounts of waste heat as a by-product. Most of this waste heat, from e.g. the exhaust gases or engine block, is transferred to the cooling water systems and is later dispersed into the sea. The idea is to recover the waste heat from the diesel engines and store it in the batteries. Two positive effects from this method would be that the batteries are operating at a more optimal temperature, giving a capacity nearer nominal level, and also an improvement of the on-board climate through heat transfer.

Since the mass of the batteries is very large, they have an enormous potential for heat storage, which should be enough, by far, to increase the temperature on-board the submarine. It has also been confirmed by previous crew members that when the batteries are heated, the on-board climate is pleasant. This is important information but needs to be confirmed with more empiric methods before one can exclude that the heat is not coming from any other process or system.

Due to the lack of space on-board the only feasible solution is to use the submarine's existing systems, which in this case means that the heat will be transferred through the battery cooling system. One emerging problem with this method is that the pole bridge, containing the cooling channel, only has a limited reach into the cell. The question arising is if it is possible to transfer enough heat to the cell using the battery cooling system.

The temperature inside the batteries varies with their state and there is a big difference in temperature if they are at rest, are being charged or being discharged. The temperature will for example rise when the batteries are being recharged and if it gets too high the batteries can be



damaged with a reduced lifetime as a consequence. However, due to the cold climate, the temperature in the batteries are often much lower than the critical limit and the cooling system is rarely used, making it possible to run heat in the circuit instead.

## ***1.2 Objectives***

The main purpose of this work is to evaluate if it is possible to accumulate heat in a lead-acid batteries by having warm water flow through the channel in the pole bridge. The essential question is how the heat will disperse inside the cell relative the time the heating is enabled.

The objective is to deliver the answer of this question together with conclusions, whether this is something worth continue working with. Beside this, a model of the cell in form of the following files will be delivered to Kockums AB to use for future work.

- Pro/Engineer CAD-file
- ANSYS ICEM geometry file
- ANSYS ICEM mesh file
- ANSYS FLUENT case and data files

## ***1.3 Limitations***

The work in this study has been concentrated to how the heat will disperse inside a battery cell and how much heat can be stored during a normal mission.

The limitations are the following:

- The cell is of maisonette type and given the name cell X.
- The existing cooling system will be used to transfer the heat.
- The cooling system will be limited to the channels inside the pole bolt and pole bridge.
- The heat is a by-product of the diesel engines.
- The used data is taken from the submarine class of Gotland.

**Due to confidential requirements from Kockums AB and FMV are all sensitive data in this report presented after using scaling factors.**

## ***1.4 Methods***

The method of this work has been according to the following steps:

- Learning enough about submarines to understand the problem.  
A submarine for military use is a very special product and to get an understanding of how a submarine works, operates and is a manufactured, internal document and previous calculations were studied. Also, an internal course at Kockums called “Submarine knowledge<sup>1</sup>” was participated. Interviews with Kockums and FMV were performed and to fulfil this background step a visit on a submarine was made.
- Analysing potential waste heat and heat storage  
Analytical calculations of the waste heat from the diesel engines and the total potential heat storage of the batteries.
- CAD-model of the cell  
Before starting to work with Pro/Engineer a meeting was held with the supplier of the cell in order to get information and drawings. These drawings and previous calculations were studied and later used as a basis for making a high-quality model. Some geometry was not reasonable to model and therefore a few simplifications had to be done.
- Meshing  
Tetra meshing was performed in ANSYS ICEM.
- Simulation  
Two different cases were set up and simulated in ANSYS FLUENT.
- Analyse  
The final step was to analyse the results from the simulations and make conclusions and comments.

## ***1.5 Outline of the thesis***

Chapter 2 introduces the different energy systems for submarine propulsion. Chapter 3 describes the numerical method and turbulence modelling. Chapter 4 describes where to find the waste heat, quantities and what the potential heat storage capacity is. The steps towards the final geometry and mesh of the model are presented in Chapter 5. In Chapter 6 the conditions and results from the simulations of the cell are reported. Chapter 7 contains the discussion and conclusions, while future work is presented in Chapter 8.

---

<sup>1</sup> Ubåtskännedom

## 2 Submarine propulsion

Kockums AB have been building submarines since 1914 and is today world leading in the technology of non-nuclear submarines. The submarines Kockums AB are producing are of a conventional type and use a system based on Stirling engines. However, the Stirling engines are the source of only one out of three ways for propulsion. Beside the Stirling engines, the submarines can also be operated by using their diesel engines or by battery propulsion.

### 2.1 *The diesel engines*

On a GTD class submarine there are two pieces of MTU diesel engines with a power of around 1MW each. The diesel engines are producing a significant amount of power which is desirable when performing a quick transfer in form of transit<sup>2</sup> or cycling<sup>3</sup> or when the batteries need to be charged. The disadvantage of the diesel engines is that they need atmospheric air to run, i.e. the submarine has to be in surface mode or snorkelling. Another disadvantage is that they create large signatures in form of visibility, noise, vibrations and heat. Most of the waste heat, from e.g. the exhaust gases or engine block, is transferred to cooling water systems and later dispersed into the sea.

### 2.2 *The Stirling engines*

Since Swedish submarines do not use nuclear power for propulsion, another system for submerged propulsion had to be developed. This system is called air independent propulsion (AIP) and is based on Stirling engines which characteristics make it possible to combust using oxygen instead of atmospheric air. The main advantage of oxygen versus air is that oxygen, in liquefied form, has a far smaller specific volume, making it possible to store in cryogenic pressure vessels on board, thus, making combustion possible while submerged.

In comparison with propulsion from the batteries the Stirling engines have many times better specific mass and overall they are a few times better when considering the complete system with weight, volume, engines etc. [1]

---

<sup>2</sup> When sailing to a certain location as quick as possible.

<sup>3</sup> Submerged propulsion by batteries until they need to be recharged, then up to snorkel depth and use of diesel engines for both propulsion and charging the batteries. When the batteries are fully charged the two steps is repeated until destination is reached.

## **2.3 Propulsion by batteries**

A submarine uses its batteries when it is cycling or submerged and need either very quiet rampage or as high speed as possible. The biggest problems with the batteries are their specific mass, which is very high, and the relatively short time it takes before the submarine needs to go to the surface and start its diesel engines for recharging.

### **2.3.1 The battery cell**

On-board GTD submarines there are two main batteries, A1 in the front and A2 in the stern. The request from FMV is to investigate a cell from the manufacturer which supplies the cells for two out of three GTD submarines. This cell, with the fictive name of cell X, exists in two different models. The differences between the two models are the dimensions and the design of them, but the mass, performance and the materials are identical making the difference in heat storage capacity negligible. Due to this fact and that over 83 % of the cells are of the maisonette type, this is the cell that is modelled.

The cells are of a wet lead-acid type especially made for submarine use and they are far bigger than a common car battery. One battery consists of a certain number of double cells which are coupled together in series to get the right amount of voltage.

A lead-acid accumulator uses lead as an active material in both the negative plates( $PbO$ ) and the positive plates ( $Pb_3O_4$ ). The material on the negative plates will during charging, in an electrolyte of sulphuric acid( $H_2SO_4$ ), lose its oxygen molecule and become pure lead while the material on the positive plates will oxidize to lead dioxide( $PbO_2$ ). While discharging the batteries the active material will pick up sulphuric acid and become lead sulphate in both types of plates.

As the cells are rather big, local temperature variations will occur and cause stratification due to density changes. To avoid this problem there is a circulation pump, pumping the electrolyte from the bottom to the top of the cell. To be able to measure for example temperature and density there is a probe together with a pole bolt and pole bridge in the top of the cell. The pole bridge contains a cooling channel which will be used to transfer the heat to the cell and is together with the circulation of great interest in this study. The electrolyte and the other components inside the cell are held together with a rubber bag enclosed by a box made of fiber glass. [2] [3]

### 2.3.2 Charging

Like all other batteries the ones on a submarine need to be recharged from time to time. A full charging process is divided into 3 parts called stage 1-, stage 2- and stage 3-charge. Figure 1 shows a charging curve that includes the 3 stages of charging with the different characteristics. During a stage 1 charge the power is constant while the current is dropping linear and the voltage is increasing. When the charging changes to stage 2 the voltage drops instantaneously to a constant level corresponding to 94% of the end voltage of stage 1, the current is decreasing more rapidly and the power is therefore also decreasing. Finally, the stage 3 charge is performed with a constant current and an increasing voltage and power.

When charging a battery an internal heat generation occurs as a result from the internal resistance and the chemical process. This internal heat generation is a function of the current and is therefore dependent of which stage of charge is executed. Figure 1 shows how the current and voltage is changing for the different stages.

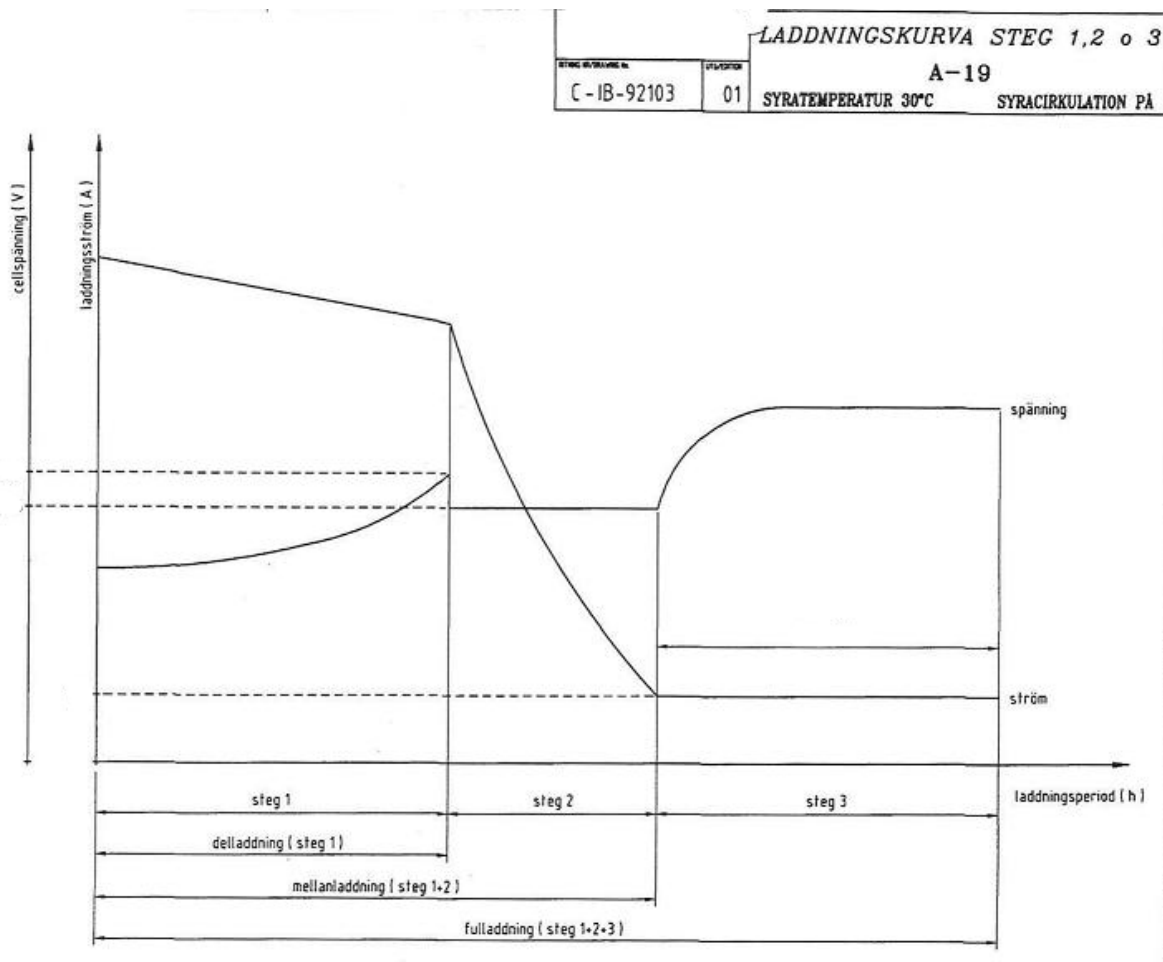


Figure 1 Charging curve for stages 1, 2 and 3 [2]

## 3 Numerical Method and Turbulence Modeling

### 3.1 Numerical Solver

The solver used in this work is ANSYS FLUENT, which uses the finite volume as numerical method.

### 3.2 Discretization method

The equations that describe the flow and heat transfer of a work volume are relatively complex partial differential equations. It is close to impossible to solve these equations analytically, therefore the method is to use CFD<sup>4</sup> programs, a technique where the work volume is divided into small control volumes and then numerically solved with iterations. This numerical method of discretization is called the finite volume method and the properties in the center of the volume are of interest. The discretization can be illustrated by the following equation for the volume V.

$$\int_V \frac{\partial \rho \phi}{\partial t} dV + \oint \rho \phi \vec{v} \cdot d\vec{A} = \oint \Gamma_\phi \nabla \phi \cdot d\vec{A} + \int_V S_\phi dV \quad (1)$$

The variables in equation (1) are explained in Table 1.

**Table 1 Description of variables in equation (1)**

Variable	Description
$\phi$	Scalar quantity
$\rho$	Density
$\vec{A}$	Surface area vector
$\Gamma_\phi$	Diffusion coefficient
$\nabla \phi$	Gradient
$S_\phi$	Source of $\phi$ per unit volume

After discretizing equation (1) for the control volume equation (2) will appear, where the variables are explained in Table 2.

$$\frac{\partial \rho \phi}{\partial t} V + \sum_f \rho_f \vec{v}_f \phi_f \cdot \vec{A}_f = \sum_f \Gamma_\phi \nabla \phi_f \cdot \vec{A}_f + S_\phi V \quad (2)$$

**Table 2 Description of variables in equation (2)**

Variable	Description
f	Face
N	Number of faces
$\phi$	Quantity convected through face
$\rho_f \vec{v}_f \phi_f$	Mass flux
A	area
V	Cell volume

<sup>4</sup> Computational Fluid Dynamics

The general equation (2) can also be described for a transient case where the equations need to be discretized not only in space but also in time. If  $F$  is a discretization for a steady-state volume, the time dependent discretization is described in (3).

$$\frac{\partial \phi}{\partial t} = F(\phi) \quad (3)$$

The first order time discretization is described in equation (4) and the second order in equation (5). The second order temporal discretization is the one used in the simulations in this study.

$$\frac{\phi^{n+1} - \phi^n}{\Delta t} = F(\phi) \quad (4)$$

$$\frac{3\phi^{n+1} - 4\phi^n + \phi^{n-1}}{2\Delta t} = F(\phi) \quad (5)$$

[4] [5] [6]

### 3.2.1 Energy equation

The main interest of this study is the heat transfer which may occur in three different ways; convection, conduction and radiation, which all are determined by the energy equation. The energy equation (6) is solving the energy transfer with respect to effective conductivity ( $k_{eff}$ ), diffusion flux ( $J$ ), viscous dissipation ( $\nu$ ) and the internal heat generation,  $S_h$ .

$$\frac{\partial}{\partial t}(\rho E) + \nabla \cdot (\vec{v}(\rho E + p)) = \nabla \cdot \left( k_{eff} \nabla T - \sum_j h_j \vec{J}_j + (\vec{T}_{eff} \cdot \vec{v}) \right) + S_h \quad (6)$$

E in equation (6) is defined as

$$E = h - \frac{p}{\rho} + \frac{v^2}{2} \quad (7)$$

where h is the enthalpy dependent on mass fraction(Y) and  $h_j$ , defined as

$$h_j = \int_{T_{ref}}^T c_{p,j} dT \quad (8)$$

and  $T_{ref}$  is 298,15K. [7] [8]

In solid regions is the energy transport equation described as equation (9), where k is the conductivity. The term directly to the left of the equal sign represents convective energy transfer due to motions in the solid. The terms to the right of the equal sign represents the heat flux due to conduction and the heat source inside the volumetric solid.

$$\frac{\partial}{\partial t}(\rho h) + \nabla \cdot (\vec{v} \rho h) = \nabla \cdot (k \nabla T) + S_h \quad (9)$$

[9]



### 3.3 The model of turbulence

There are many different models to calculate the effect from turbulence. The models are working towards the same objective but in different ways, which makes some models more appropriate to use for a certain problem than others. Choosing the “wrong” model will have a negative effect on the results and it might also cause the solver to diverge. Since the simulations are long transient cases the amount of iterations before reaching convergence has been a crucial factor when deciding what model to use. Trial and error showed that the k-ε realizable model fitted the problem well and had the advantage of reaching convergence fast and was therefore chosen.

#### 3.3.1 K-ε realizable model

The k-ε models are often the standard choice in the industry since it is robust, relatively quick and easy to work with because only a few parameters has to be set before starting the simulation. Another advantage of the k-ε models, and especially the realizable model, are that they give good results for a wide range of flows. The realizable k-ε model has previously been reported to give reasonable results for many types of flows including rotation, boundary layer with pressure gradients, separation and recirculation.

The k-ε realizable model is presented in (10) - (14) with a description of the model parameters in **Table 3**.

$$\frac{\partial}{\partial t}(\rho k) + \frac{\partial}{\partial x_j}(\rho k u_j) = \frac{\partial}{\partial x_j} \left[ \left( \mu + \frac{\mu_t}{\sigma_k} \right) \frac{\partial k}{\partial x_j} \right] + G_k + G_b - \rho \varepsilon - Y_M + S_k \quad (10)$$

$$\frac{\partial}{\partial t}(\rho \varepsilon) + \frac{\partial}{\partial x_j}(\rho \varepsilon u_j) = \frac{\partial}{\partial x_j} \left[ \left( \mu + \frac{\mu_t}{\sigma_\varepsilon} \right) \frac{\partial \varepsilon}{\partial x_j} \right] + \rho C_1 S_\varepsilon - \rho C_2 \frac{\varepsilon^2}{k + \sqrt{V \varepsilon}} + C_{1\varepsilon} \frac{\varepsilon}{k} C_{3\varepsilon} G_b + S_\varepsilon \quad (11)$$

$$C_1 = \max \left[ 0.43, \frac{\eta}{\eta + 5} \right] \quad (12)$$

$$\eta = S \frac{k}{\varepsilon} \quad (13)$$

$$S = \sqrt{2 S_{ij} S_{ij}} \quad (14)$$

**Table 3 Description of variables for equation (10) - (14)**

<b>Variable</b>	<b>Description</b>
$G_k$	Generation of kinetic energy due to velocity
$G_b$	Generation of kinetic energy due to buoyancy
$Y_M$	Fluctuating dilatation
$C$	Constants
$\sigma$	Turbulent Prandtl number
$S$	User-defined source terms

[10]

### ***3.4 The SIMPLE algorithm***

SIMPLE is an abbreviation for Semi-Implicit Method for Pressure-Linked Equations and is a method for iterative solution to the pressure – velocity coupling. This algorithm is based on the following steps: First the momentum equations are solved using a guessed pressure field to get initial values of the velocity components. After this, a correction equation is solved for the pressure and velocity fields resulting in new starting values for the transport equations. This procedure is repeated using the updated values until mass conservation is achieved. [11]

## 4 Available waste heat and potential heat storage capacity

### 4.1 Waste heat from the diesel engines

The submarine class Gotland has two diesel engines that are producing significant amounts of waste heat as a by-product. Most of the waste heat, from e.g. the exhaust gases or engine block, is transferred to cooling water systems and later dispersed into the sea. The available heat in these two locations is described in the sections below.

#### 4.1.1 Exhaust gases

The MTU diesel engines on board a submarine of the GTD class are running with a lambda value of 2 and producing exhaust gases with a mass flow of 2,4kg/s at a temperature of 550°C. Due to temperature restrictions for the rubber in the valves, and to keep down the heat signatures, the exhaust gases needs to be cooled to a temperature of 250°C, presently this heat is not utilized.

The diesel fuel used for the combustion will be assumed to be  $C_{12}H_{23}^5$  and since the engine is running with a lambda value of 2, the mixture is lean and the chemical composition can therefore be calculated according to equation (15). By solving the following equations and using the deliverables in the chart for specific heat in Figure 2 the available energy can be determined.

$$C_a H_b + \lambda \cdot \left(a + \frac{b}{4}\right) \cdot (O_2 + 3,773N_2) = aCO_2 + \frac{b}{2}H_2O + (\lambda - 1) \cdot \left(a + \frac{b}{4}\right)O_2 + 3,773\lambda \left(a + \frac{b}{4}\right)N_2 \quad (15)$$

$$\frac{x_{H_2O}}{x_{CO_2}} = \frac{n_{h_2o}/n}{n_{co2}/n} \quad (16)$$

$$P = \dot{m} \cdot cp \cdot (T_1 - T_2) \quad (17)$$

[12]

---

<sup>5</sup> Reference [25]

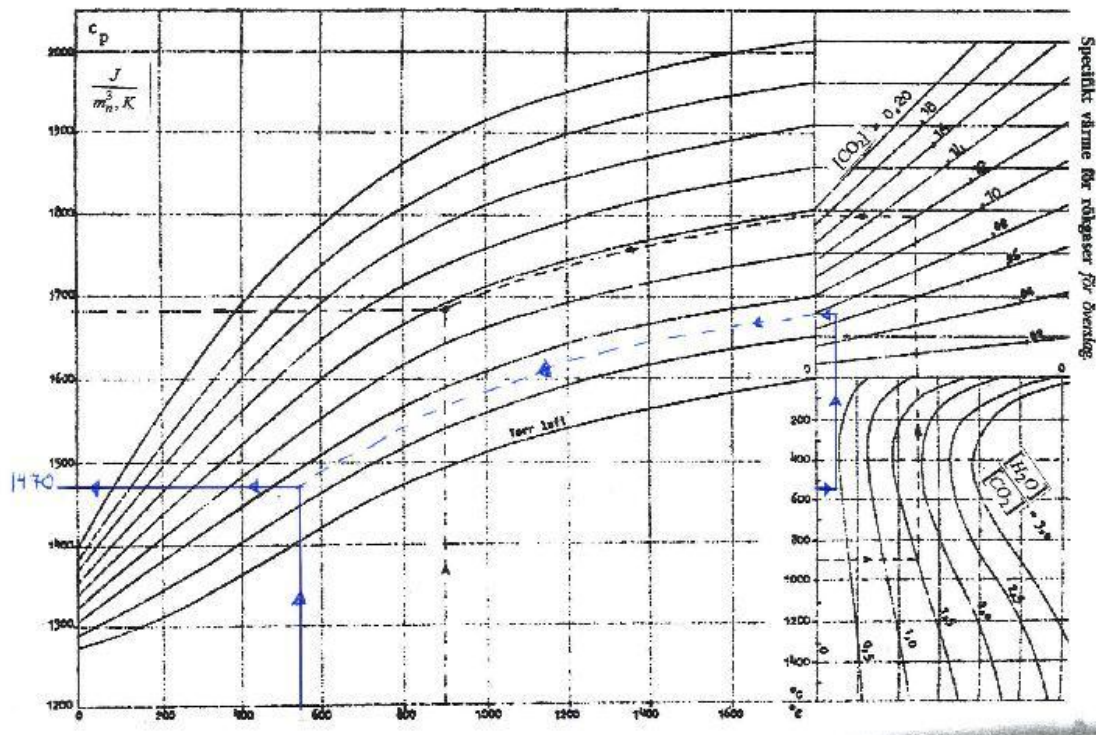


Figure 2 Chart for specific heat of flue gases [13]

The total available heat when the two engines are running at full power is 2 times 1037kW, i.e. 2074kW.

#### 4.1.2 Cooling water

The cooling water is used to transfer heat away from the block of the diesel engines. Most of the waste heat is released to the ocean, however, a hot water circuit is exchanging about 56kW from the system for use in air conditioners and similar systems. The water in this hot water circuit has a delivery temperature of 50°C, and a return temperature of 35°C after passing by the applications in the system. [14]

To answer the question if there is more available heat besides the 56kW already in use, estimation with equations (18) - (19) and data according to Table 4 is performed.

Table 4 MTU diesel engine data

Power( $P_{\text{shaft}}$ )	1040kW
Efficiency( $\eta$ )	0,3
Heat effect in exhaust gases( $Q_{\text{exhaust}}$ )	1037kW

$$P_{total\_loss} = \frac{P_{shaft}}{\eta \cdot (1 - \eta)} \quad (18)$$

$$P_{cooling} = P_{total\_loss} - P_{exhaust} \quad (19)$$

The available heat when both engines running at full power are 2 times 1390kW, which equals 2,8MW. This is significantly more than the already recovered waste heat. It is preferable to use the cooling water as a source for the waste heat since it is much easier to work with water than with flue gases, due to corrosion problems.

Chapter 4.3 will show that the energy available in the cooling system is much more than needed and therefore further work will be under the assumption that the heat is taken from the cooling system.

#### 4.2 Potential heat storage in the batteries

The heat storage potential is calculated by equation (21), which is dependent on the average specific heat for the whole cell. The data for what and how much one cell contains of a certain material and the specific heat of the materials is listed in Table 5. The energy storage potential is dependent on the possible temperature increase. In this case the temperature is assumed<sup>6</sup> to be 7°C at the start and that it is elevated to 45°C during the process.

**Table 5 Mass and specific heat for one cell [15]**

Substance	Mass(kg)	C <sub>p</sub> (kJ/(kgK))
Lead(Pb)	272,5	0,13
Copper(Cu)	52,5	0,39
Sulphuric acid(H <sub>2</sub> SO <sub>4</sub> )	49	1,38
Water(H <sub>2</sub> O)	74,5	4,18
Other materials	36,5	1,6
Total/Average	485	1,02

$$c_{p,avg} = (\sum m_i \cdot c_{p_i}) / m_{total} \quad (20)$$

$$Q = m \cdot c_{p,avg} \cdot \Delta T \quad (21)$$

<sup>6</sup> The assumption is based on information from co-workers with technical experience from submarines and with the condition that the battery is not charging or discharging.

One cell has a heat storage potential of 18,8 MJ which will give a great amount of energy storage when all cells on-board are summarized.<sup>7</sup>

By comparison, a regular accumulator tank for a villa has energy storage of about 420MJ, which is much less than the potential storage in the batteries. This estimation is calculated by assuming a tank with 2 m<sup>3</sup> of 70°C water and a reference temperature of 20°C. In the calculation a specific heat of 4,18 kJ/(kg K) and a density of 1000 kg/m<sup>3</sup> is used. [16]

$$Q_{acc} = m \cdot c_p \cdot \Delta T = 2000 \cdot 4,18 \cdot (70 - 20) = 418MJ \approx 0,42GJ$$

### **4.3 Potential transfer of heat from the pole bridge**

In earlier calculations of the cooling effect from the pole bridge, the manufacturer has been using an unverified constant of 24W/(bridge °C). This constant is dependent on the temperature difference between the electrolyte and the cooling water, and has therefore the biggest value of transferred heat when the electrolyte temperature is at its lowest point, in this case 7°C, and the smallest value when the electrolyte temperature is 30°C. [17]

Equation (22) is describing the transferred heat at a specified time were  $N_{cells}$  is the number of cells,  $N_{bridges}$  is the number of bridges,  $P_{bridge}$  the heat transfer constant from previous calculations and  $\Delta T$  the temperature difference between the electrolyte and cooling water.

$$Q_{total} = N_{cells} \cdot N_{bridges} \cdot P_{bridge} \cdot \Delta T \tag{22}$$

The largest value of transferred heat is 912W/bridge, which multiplied by all bridges and all cells on board gives a total value of transferred heat much lower than available. This indicates that the limiting factor is the available time for the heating process.

---

<sup>7</sup> For full details go to Appendix A2

## 5 Geometry and Mesh Generation

### 5.1 Program

The program that has been used for creating the geometry is PTC's Pro/Engineer (PTC, Needham, MA) and ANSYS ICEM 12.1 (Ansys Inc., Canonsburg, PA).

### 5.2 Geometry

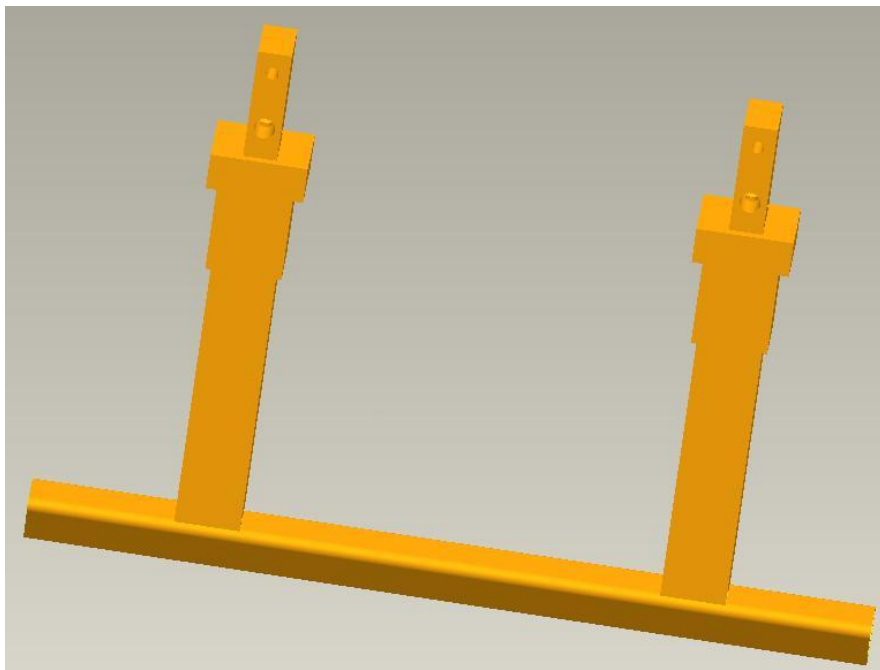
To create the geometry a 5 step process has been as follows:

1. Studying data and drawings from the supplier.
2. Creating the geometry in Pro/engineer based on this information
3. Making simplifications and calculating average material data to reduce the number of elements in the mesh.
4. Modify the geometry after decided simplifications.
5. Tetra meshing.

#### 5.2.1 Geometry generation

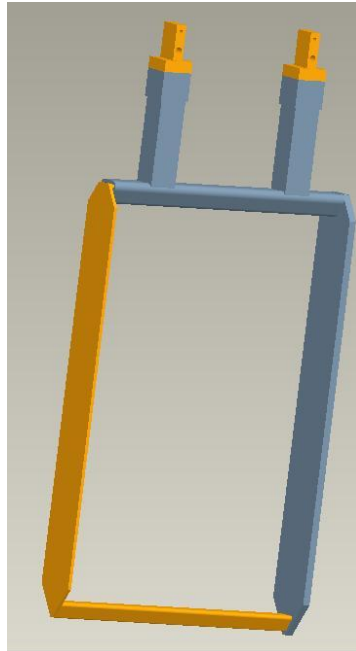
The geometry has been created part for part and then put together in an assembly that includes all the solids in the cell. This section will graphically show the important parts and how it is assembled.

Figure 3 shows the copper core of the pole bolt and pole bridge. There are drilled channels inside the pole bolts and in the bridge there is a molded channel with the shape of a triangle with rounded corners. The water is led down through the first pole bolt, reaching the bridge with a 90 degree direction change. The main flow line is over the pole bridge and up and out in the other pole bolt, but there are also some spaces in the pole bridge outside the bolts where some movement will appear.



**Figure 3 The copper core of the pole bolts and pole bridge**

The copper core of the pole bolt and pole bridge is then added with a lower pole bridge, which is located between the two plate packages and connected to the upper pole bridge with two copper plates. Due to the chemical reaction with the electrolyte, all metal in contact with the acid needs to have a coating of lead which can be seen in Figure 4.



**Figure 4 Copper core partly coated with lead**

The plate packages are modeled as cubic volumes (explained in Chapter 5.3) and are placed between and under the pole bridges illustrated as the free space in the middle in Figure 4. Figure 5 shows at the left an assembly of the complete cell without the rubber bag and fiber glass box and to the right the same cell but this time showing the fiber box. Since the geometry is symmetrical, by a wall separating the two single cells, the geometry will later on be cut into half.

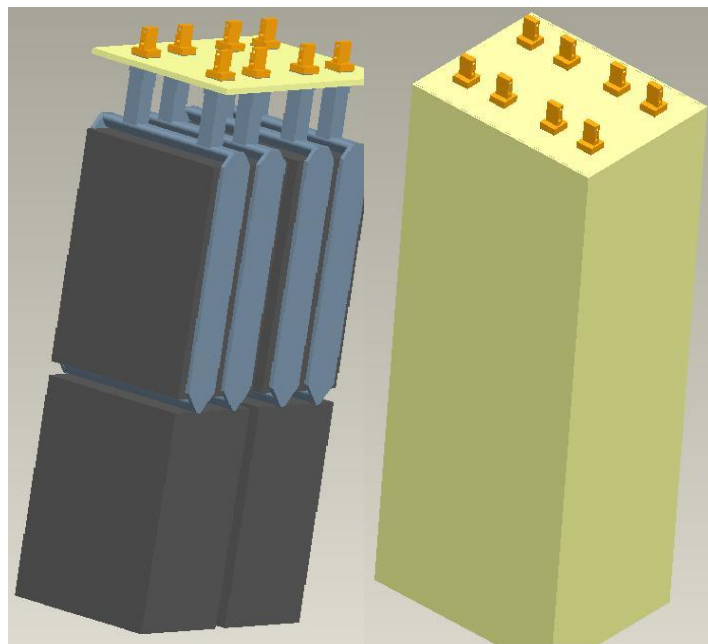


**Figure 5 Geometry of the cell**



### 5.3 Simplification of the geometry

#### 5.3.1 Plate packages

The plate package in the cell consists of a couple of different materials. There are positive plates made of lead, negative plates made of a copper core with a layer of lead, separators made of a plastic material and sulphuric acid between and around all the solids. In each double cell there are 4 plate packages with data according to Table 6.

**Table 6 Data for the materials inside the plate package [18] [19]**

	Lead(Pb)	Copper(Cu)	Plastic	Sulphuric acid(H <sub>2</sub> SO <sub>4</sub> )
C <sub>p</sub> [kJ/(kgK)]	0,128	0,39	1,6	1,38
λ [W/(mK)]	35,2	398	0,23	0,26
m [kg]	96,8	13,6	1	49,4(total)
ρ [kg/m <sup>3</sup> ]	11200	8950	1410	1300

##### 5.3.1.1 Acid outside the plate package

The electrolyte is both in between and around the plate packages. Since the only known data is the total amount of electrolyte, the amount of electrolyte between the plates is calculated by subtracting the “free” volume around the packages by the total volume.

The, so called, free volume and the mass of the electrolyte between the plates is calculated in Appendix A3 with results according to Table 7.

**Table 7 Masses and volumes for the electrolyte**

	Free	Between plates	Total
m[kg]	11,3	38,1	49,4
V[dm <sup>3</sup> ]	8,7	29,3	38

### 5.3.1.2 Calculating the average specific heat

The specific heats for the different materials are known, but the specific heat for the mixture of the electrolyte and the average specific heat for whole plate packages are not. Since the specific heat has the unit J/(kgK), is it mass dependent and the average value is calculated by summing the mass fractions multiplied with the specific heat of the different materials according to equation (23).

$$cp_{avg} = \sum \mu_i \cdot cp_i \quad (23)$$

The given data and the results from equation (23), details can be found in Appendix A4, are presented in Table 8.

**Table 8 Mass fractions and specific heat for the materials in the plate packages [17]**

	C <sub>p</sub> [kJ/(kgK)]	m[kg]	μ[-]
<b>Electrolyte contents</b>			
Sulphuric acid(H <sub>2</sub> SO <sub>4</sub> )	1,38	15,1	0,395
Water(H <sub>2</sub> O)	4,18	23	0,605
<b>Result</b>			
Electrolyte	3,074	38,1	
<b>Contents of the package</b>			
Lead(Pb)	0,128	96,8	0,647
Copper(Cu)	0,39	13,6	0,091
Plastic	1,6	1	0,0067
Electrolyte	3,074	38	0,255
<b>Result</b>			
Average plate packages value	0,913		

### 5.3.1.3 Calculating the average density

Density can be calculated according to (24) were the total mass of the packages of one cell is 149,5kg and since there are 4 packages in every cell which gives one plate package has a mass of 37,4 kg. The volume is 0,01104m<sup>3</sup> per package and the plate package has an average density of 3385 kg/m<sup>3</sup>.

$$\rho = \frac{m}{V} \quad (24)$$

### 5.3.1.4 Calculating the total thermal conductivity

When calculating the total thermal conductivity it is important to consider that the new fictive material will be of anisotropic nature since heat transfer is not the same in the direction along the plates as it is through the plates. The thermal conductivity can be calculated in analogy with electric resistance and are for parallel arrangement inversely proportional to parallel resistance in electricity.

The analogy is explained with Figure 6 and the following equations where  $Q$  is the heat flux,  $\lambda$  the thermal conductivity,  $\Delta T$  the temperature difference,  $b$  the length in the heat flux direction,  $A$  the area  $90^\circ$  from the heat flux direction and  $R$  is the resistance.

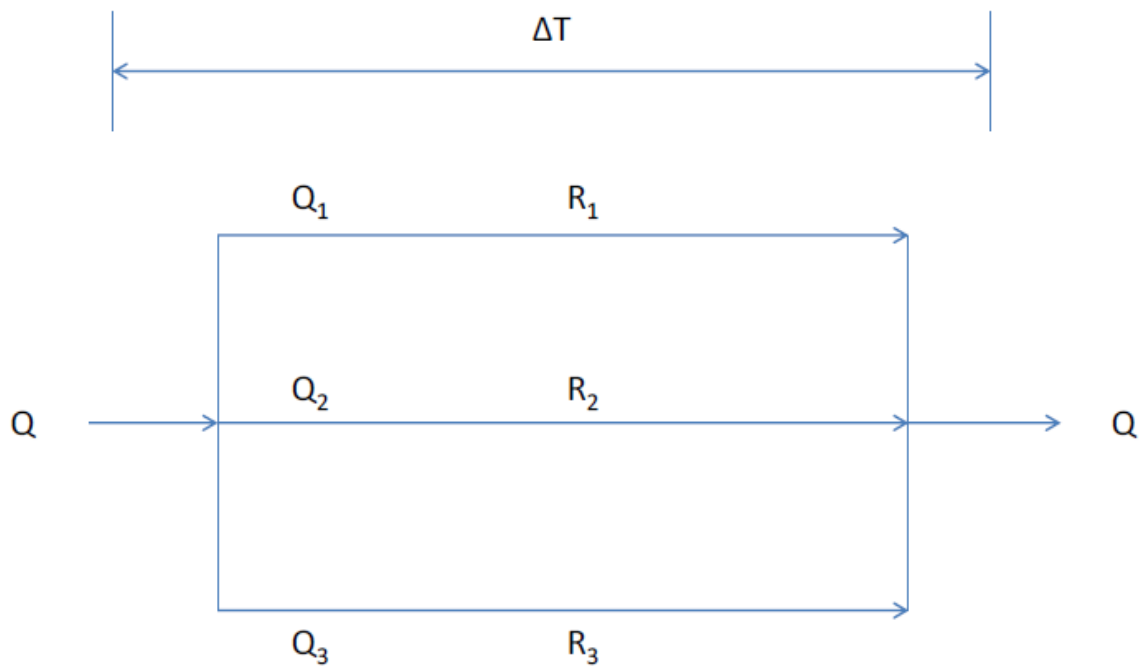


**Figure 6 Analogy between electric resistance and heat transfer**

$$Q = \lambda A \frac{\Delta T}{b} \quad (25)$$

$$R = \frac{b}{\lambda A} \quad (26)$$

$$\Rightarrow Q = \frac{\Delta T}{R} \quad (27)$$

For parallel structure:

$$Q = Q_1 + Q_2 + Q_3 \quad (28)$$

$$\frac{1}{R} \cdot \Delta T = \frac{\Delta T}{R_1} + \frac{\Delta T}{R_2} + \frac{\Delta T}{R_3} \quad (29)$$

$$R = \frac{1}{\frac{1}{R_1} + \frac{1}{R_2} + \frac{1}{R_3}} = \frac{R_1 \cdot R_2 \cdot R_3}{R_1 \cdot R_2 + R_1 \cdot R_3 + R_2 \cdot R_3} \quad (30)$$

$$\frac{b}{\lambda \cdot A} = \frac{\frac{b_1}{\lambda_1 \cdot A_1} \cdot \frac{b_2}{\lambda_2 \cdot A_2} \cdot \frac{b_3}{\lambda_3 \cdot A_3}}{\frac{b_1 b_2}{\lambda_1 A_1 \lambda_2 A_2} + \frac{b_1 b_3}{\lambda_1 A_1 \lambda_3 A_3} + \frac{b_3 b_2}{\lambda_3 A_3 \lambda_2 A_2}} \quad (31)$$

In the directions where the plates will be in a serial arrangement the thermal conductivity is calculated by equation (32).

$$\frac{\delta_{total}}{\lambda_{total} \cdot A} = \sum \frac{\delta_i}{\lambda_i \cdot A_i} \quad (32)$$

[20] [21]

Distances, directions and arrangements of the plates are according to Figure 7.

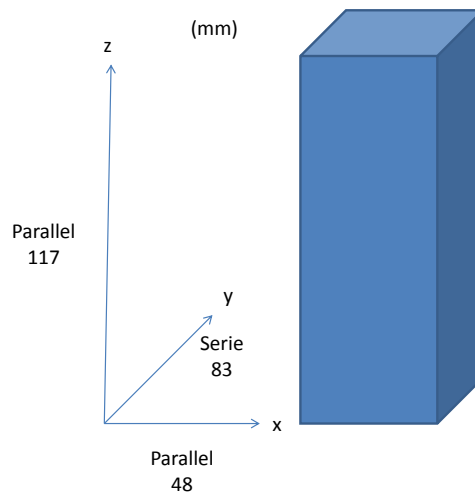


**Figure 7 Distances and directions of the plate packages**

The plate package consists of the same amount of positive and negative plates with separators and electrolyte between. The y-direction is the only direction with a serial arrangement which has a structure of repeated groups with positive and negative plates, and separators including electrolyte with thicknesses according to Figure 8. One group is illustrated by a thickness of 50 units(u).

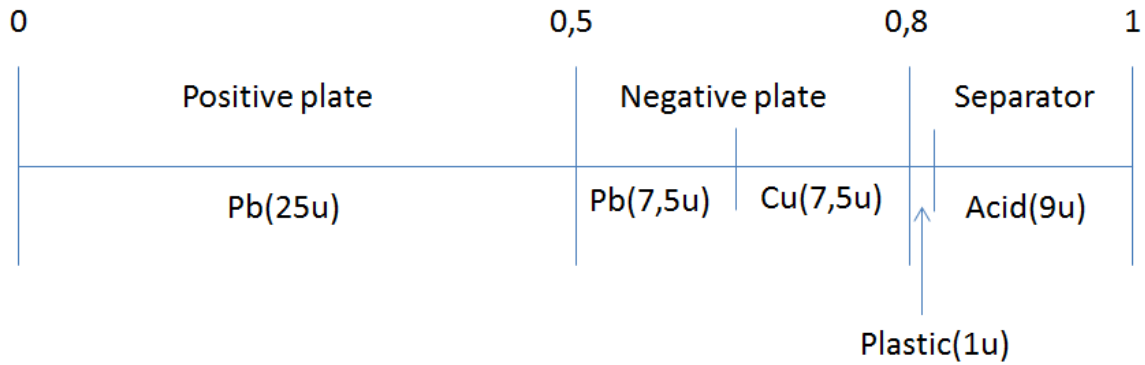


**Figure 8 Illustration of thickness and units of one group [22]**

**Table 9 Thicknesses of the different materials in one group**

	Thickness ( $\delta$ ) [mm]
Lead(Pb)	2,13
Copper(Cu)	0,49
Separators(plastic)	0,066
Electrolyte	0,59
<b>1 group</b>	<b>3,44</b>

The thermal conductivity for the different directions is presented in Table 10 where the y direction is calculated with equation (32) and x- and z-direction calculated with equation (31).

**Table 10 Anisotropic thermal conductivities for the plate packages**

	X	Y	Z
$\lambda$ [W/(mK)]	82,3	1,31	38,07

### 5.3.2 Lower pole bridges

Between the two plate packages there is another pole bridge much alike the ones in the top, but without any heating/cooling fluid. Instead the channel is just sealed with air inside and enclosed by 5mm of lead surrounding 3 mm of copper with a shape of a triangle.

To keep down the amount of mesh elements this pole bridge is also simplified and assumed to have isotropic properties. Equation (23), (24) and (32) is used to determine the density, specific heat and thermal conductivity for the new material.

**Table 11 Data for the lower pole bridge [18]**

	Air	Lead	Copper	Total/Average
m[kg]	$1,57 \cdot 10^{-4}$	2,16	0,82	2,98
$V[m^3] \cdot 10^{-4}$	1,3	1,93	0,917	4,15
$\rho[kg/m^3]$	1.205			7186
$C_p[kJ/(kgK)]$	1,005			0,2
$\delta[mm]$	14,7	2*5=10	2*3=6	30,7
$\lambda[W/(mK)]$	0,0257	35,2	398	<b>0,054</b>

### 5.3.3 Vertical plates connecting the pole bridges

In Figure 4 the vertical plates are shown and because of their thin thicknesses of the different materials, 2 times 3mm of lead and 1 time 5mm of copper, the size of the mesh elements has to be very small and the total amount of elements tends to become very large. To decrease simulation time the vertical plates are also modelled, as previous simplifications, as one uniform material instead of three layers. The complete calculation is found in Appendix A8 and the results are presented in Table 12.

**Table 12 Anisotropic thermal conductivities for the vertical plates**

	X	Y	Z
$\lambda[\text{W}/(\text{mK})]$	275,2	60,1	200,1

The density of the plates is dependent of the volume fraction of each component, and the average density for the material is therefore calculated as a volume weighted averaged according to equation (34). As before, the average specific heat is weighted with their mass fraction according to equation (23).<sup>8</sup>

$$\mu_v = \frac{V_i}{V_{total}} \quad (33)$$

$$\rho = \sum \mu_{v,i} \cdot \rho_i \quad (34)$$

Table 13 shows the results for the density and specific heat for the vertical plates.

**Table 13 Data for the vertical plates**

	Lead	Copper	Total/Average
$V[\text{m}^3] \cdot 10^{-4}$	3,12	2,59	5,7
$\mu_v [-]$	0,545	0,455	
$\rho[\text{kg}/\text{m}^3]$			<b>10176</b>
$m[\text{kg}]$	3,5	2,3	5,8
$\mu_m [-]$	0,6	0,4	
$C_p[\text{kJ}/(\text{kgK})]$			<b>0,234</b>

<sup>8</sup> Complete calculations in Appendix A8

## 5.4 Mesh generation

Figure 9 shows the geometry after editing in form of simplifications and adding of a pipe illustrating the circulation of the electrolyte.

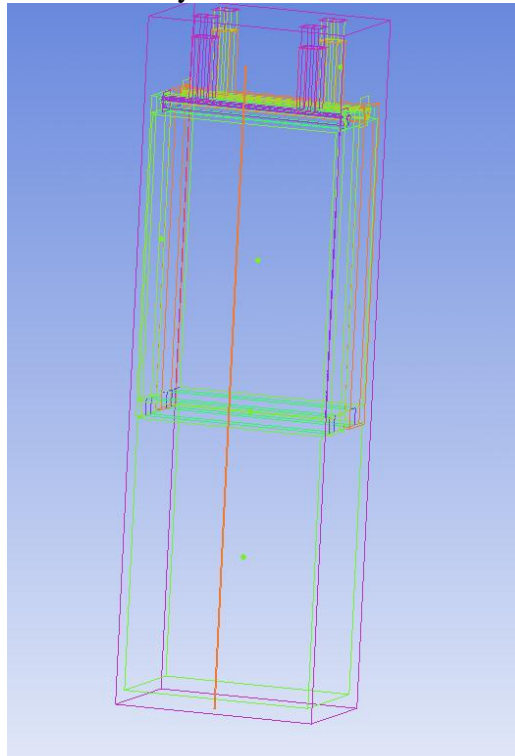


**Figure 9 Geometry after final editing**

### 5.4.1 The meshing method

The 3D cell has a rather complicated geometry making it more efficient to use the tetra mesh type. The Robust (Octree) method has been used as meshing method, which is based on a spatial subdivision algorithm and is working with a top-down system. The method is not requiring a surface mesh to calculate from since it is being created in the Octree process. The main advantage of the Robust (Octree) method is that it allows fast computation since the algorithm is trying to use larger elements where it is possible. The method starts with creating relatively large tetrahedrons that together embraces the entire volume. This tetra is then subdivided until all criterions are satisfied. Figure 10 illustrates the surface mesh of the copper core inside the pole bolt and pole bridge while Figure 11 shows a wider perspective of the top part of the cell. [5]



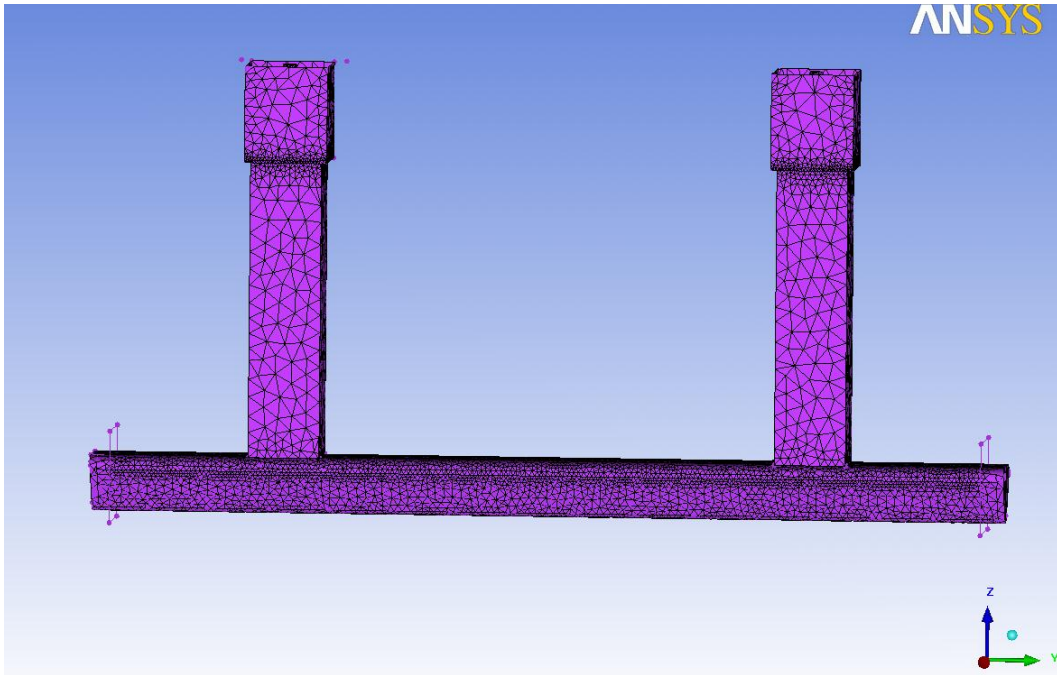


**Figure 10** Surface mesh of the copper core inside the pole bridge and pole bolt

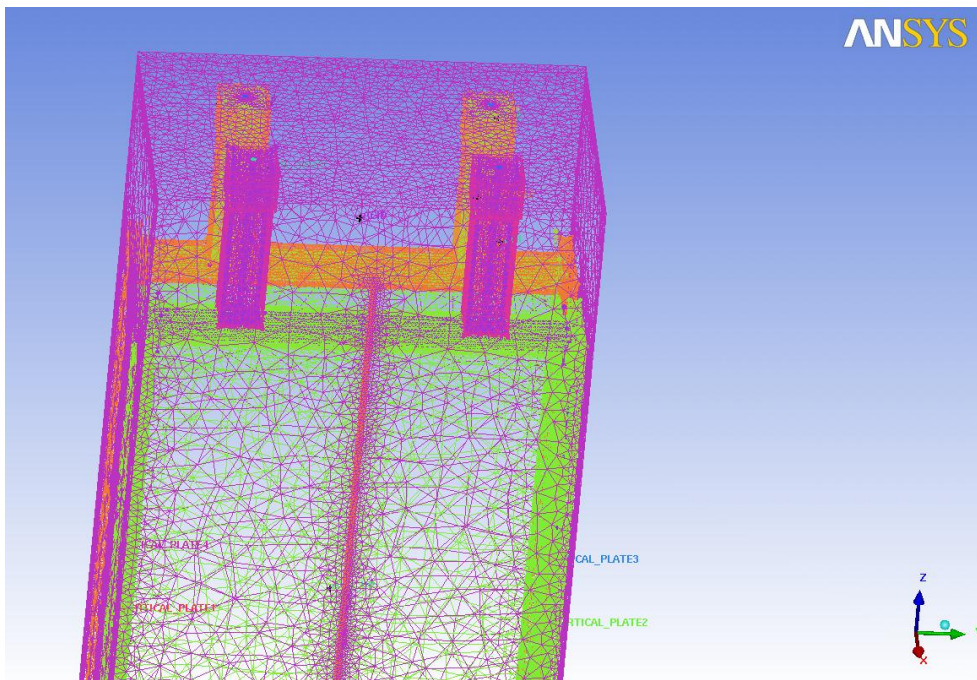


**Figure 11** Shell mesh of the upper part of the cell

## 6 Simulation of heat absorption in a battery cell

### 6.1 General conditions

#### 6.1.1 Computational settings

The cell in the simulation is a double cell which has been split in half due to its symmetry and assumed to be in the middle of the battery pack making the assumption of isolated walls believable. The top of the cell is set to be isolated while the bottom of the cell is in direct contact with the hull of the submarine and is therefore of the same temperature as the surrounding water. In order to circulate the electrolyte inside the cell a mammoth pump is running with the mission to transport the electrolyte from the bottom to the top. Table 14 is summarizing the settings and conditions for both cases.

**Table 14** General simulation settings

Solver	Pressure-Based
Time	Transient
Gravity	-9.82 m/s <sup>2</sup>
Turbulence model	k-ε realizable
Near-Wall Treatment	Enhanced Wall Treatment
P-v coupling	SIMPLE
Spatial discretization	Second Order
Transient Formulation	Second Order Implicit
Under-Relaxation Factors Energy	0.5
BC cell walls + top	Isolated
BC bottom	$T_{\text{constant}} = 7^{\circ}\text{C}$
Water flow inlet	$\dot{m} = 0,01\text{kg} / \text{s}, T = 45^{\circ}\text{C}$
Mammoth pump	40 litre/hour, (fan setting: $\Delta P = 2400\text{ Pa}$ )
All Cell zones at $T_0$	$T = 7^{\circ}\text{C}$
Time step(0 → 1,5s)	0,001s
Time step(1,5s → 5h)	10s
Iterations per time step	30

### 6.1.2 Monitor points and contour planes

In the simulation program it is possible to save data in a couple of different ways. One way is to save all data at specific time intervals but each data file is in this case of a size about 0,5GB which makes it impossible to store too often. To get the exact information at every time step it is instead possible to create monitor points that saves the temperature at a specific location in a text file that does not take up much disk space. The monitor point data is later on plotted versus the time and gives a clear view of how the temperatures have increased over time. The monitor points are placed according to Table 15 and Figure 12.

**Table 15 Description of the location of the monitor points**

P1	The electrolyte in top
P2	In the middle of the upper plate package
P3	Electrolyte between the two plate packages
P4	In the middle of the lower plate package
P5	Electrolyte beside the plate package 1/3 down

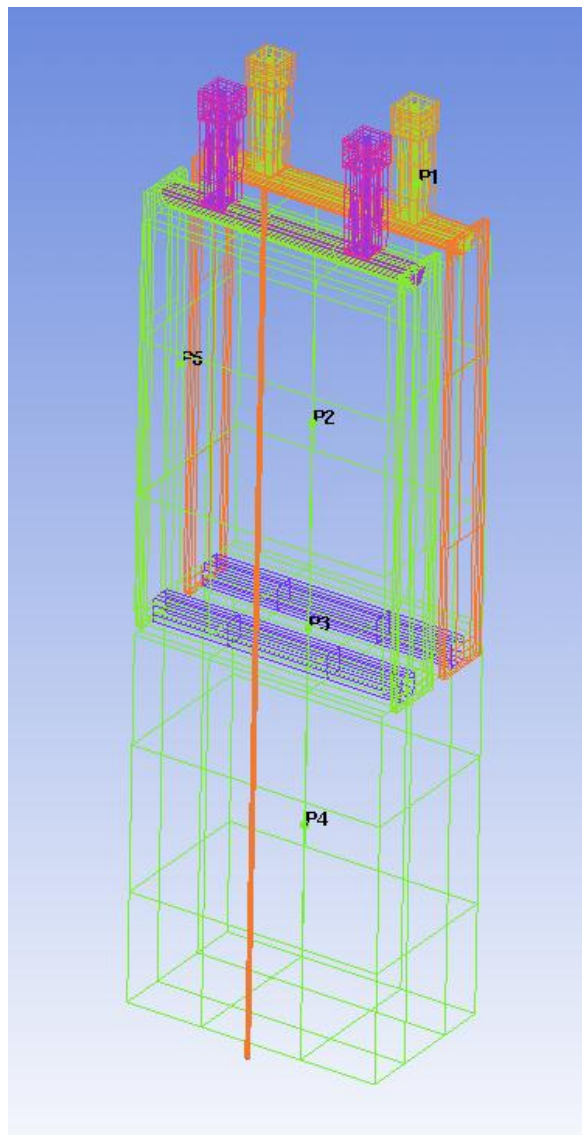


**Figure 12 Monitor points**

The contour figures presented in the results are of three different types, either a plane in the middle of the cell in x and y direction or a figure describing the temperature of the electrolyte in contact with the box. The x and y plane are described in Figure 13 where they are illustrated as the green planes in the middle.

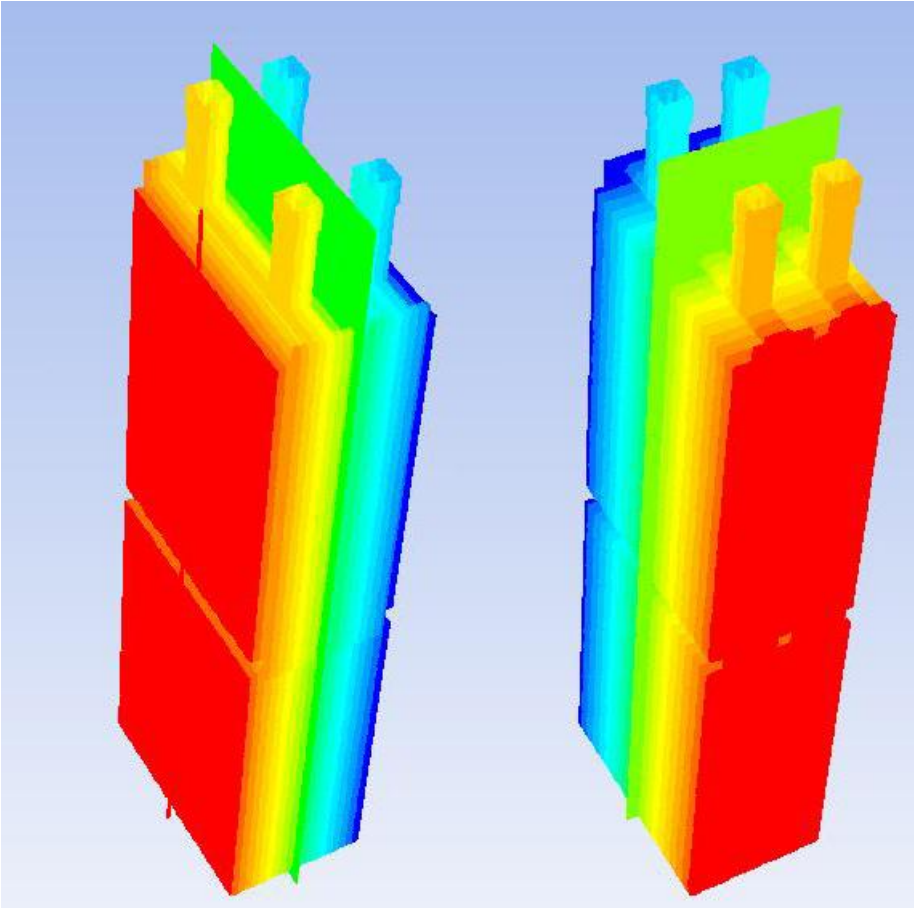


**Figure 13 Monitor planes**

## 6.2 *Fictive mission to simulate*

A fictive mission has been invented, to make the cases for simulation as realistic as possible, as following.

It is winter in Sweden, a submarine of Gotland class has been to berth in Karlskrona harbour for a couple of days when they get their mission to monitor the traffic of ships outside the Lithuanian harbour of Klaipeda. When the submarine leaves Karlskrona harbour next day the temperature in the batteries is of the same temperature as the water, 7°C. By the time the submarine is leaving Karlskrona harbour they are facing a transfer which will consist of the following 3 steps.

1. The submarine dives when it reaches open water and uses its batteries for propulsion with a discharge of 400A/battery for a couple of hours. When the rest capacity for the batteries is down to 40-50 %, they need to be recharged. At this point the batteries still have a temperature of 7 degrees Celsius.
2. The submarine rises to snorkelling level and starts its diesel engines and stage 1 charging of the batteries. They will also start their new heating system of the batteries which uses the waste heat from the diesel engines. This charging represents a constant power of 320kW, the rest is used for propulsion. An average cell voltage of 0,47V which will give a charging time of a few hours.
3. When stage 1 charging is completed the submarine is still using the diesel engines for propulsion and heating the batteries but changes to a stage 2 charge with a constant cell voltage of 0,47V and a current that starts at 280A and dropping by half every hour to 60A which will take 2 hours and 20 minutes.

After step 3 of transfer the submarine reaches the location where the AIP mission starts. When the mission is completed and the target is to get home to Karlskrona harbour again, the three steps above are repeated.

The simulation case 1 will be according to the conditions of the second step of the transfer and case 2 the third step of the transfer. [23]

### 6.3 The internal heat generation

When the batteries are being charged the temperature will rise due to the internal resistance and the chemical process. By combining equation (35) - (37), where  $U_0$  is the internal voltage, the internal heat generation can be predicted.

$$dQ = I \cdot dU \cdot dt \quad (35)$$

$$dU = U - U_0 \quad (36)$$

$$I = \frac{P}{U} \quad (37)$$

Where  $U_0$  is the internal voltage which is density dependent.

The given information and the results of the internal heat generation for the different charging properties are presented in Table 16 where the density is taken from Figure 14.

During stage 2 the voltage will drop by half every hour and an average voltage is therefore calculated by weighing the voltages against the time fraction. The previous discharge is assumed to be the discharge capacity before stage 1 minus the capacity of stage 2.<sup>9</sup> [17] [2]

**Table 16 Data and results of heat generation for stage 1 and stage 2 charge**

	<i>Stage 1 charge</i>	<i>Stage 2 charge</i>
P[W/cell]	190	67,84
U[V]	0,47	0,47
I[A]	405,2	144.34
Previous discharge[Ah]		
V[m <sup>3</sup> ]	0.108	0,108
$\rho$ [kg/m <sup>3</sup> ]	1,19	1,285
dQ[W/cell]	182	30,1
Heat generation[W/m <sup>3</sup> ]	<b>1693</b>	<b>280</b>

<sup>9</sup> Complete calculations in Appendix A10

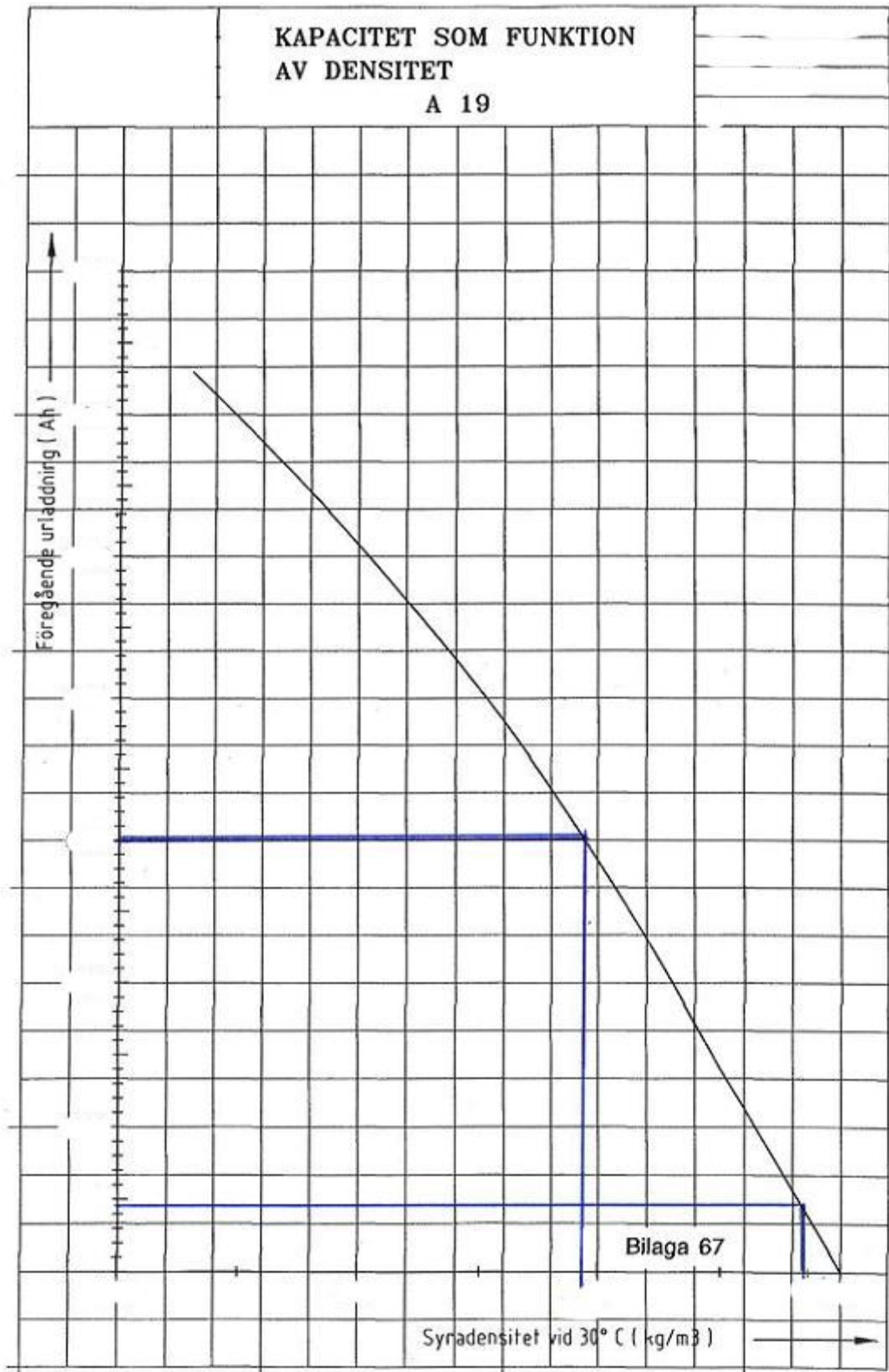


**Figure 14 Capacity as function of density of electrolyte [24]**

## 6.4 Case 1: Heating combined with stage 1 charging

### 6.4.1 Conditions

- Heat generation in both plate packages of  $1693\text{W/m}^3$ .
- All zones beside the water have a starting temperature of  $7^\circ\text{C}$ .

### 6.4.2 Results and comments

Figure 15 shows how the temperature varies over time in the monitor points, which are defined in Figure 12 and Table 15. The temperature is increasing rapidly in the electrolyte in the top of the cell to a temperature of 30 degrees in just 30 % of full time. The deeper down in the cell the monitor point is located, the lower is the temperature, except P5 which can be explained by the cold electrolyte that has been transferred to the top by the pump is, by natural convection, passing monitor point P5 on the way down. The fact that P4 is much lower than P2 shows that the direct heating from the pole bridge to the upper plate package is rather big.

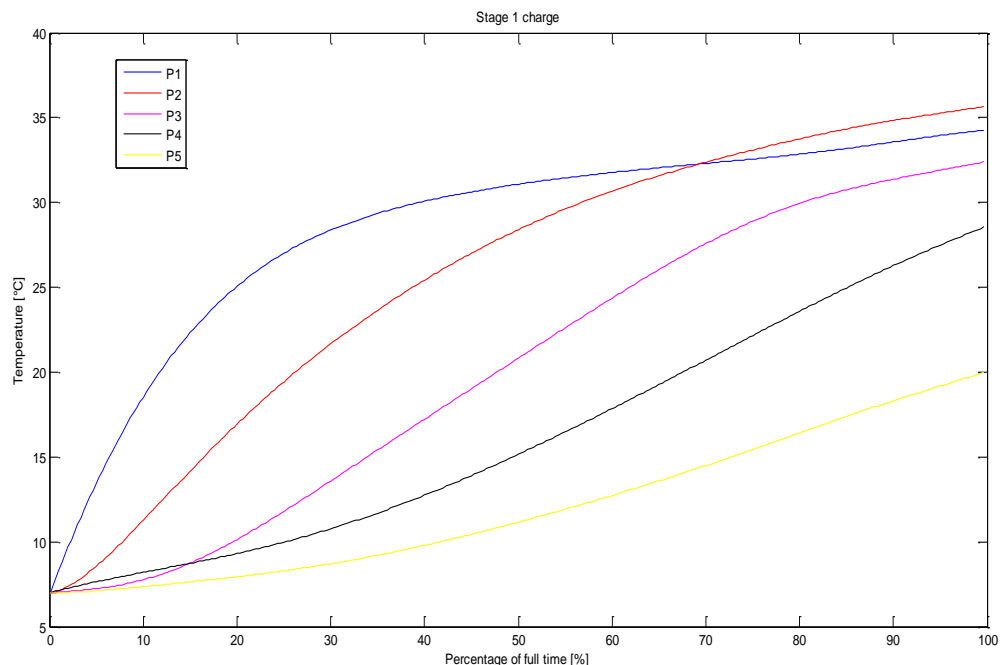


**Figure 15 Temperature versus time during stage 1 charge**

After 70 % of full time the temperature in the upper plate package is higher than the temperature of the top electrolyte. This indicates that the internal heat generation plus the heat transfer from the pole bridge has a larger effect than the pole bridge at this point delivers to the electrolyte. The delivered heat to the electrolyte is decreasing over time due to a smaller  $\Delta T$  when the electrolyte is being heated.

The temperature is very different in different positions of the electrolyte and after 40 % of full time is the biggest temperature difference, 20,5 degrees, is observed, between P1 and P5. This will affect the densities and maybe create stratification, especially if the circulation of the acid is not good enough. It can be seen that the temperatures in the different monitor points all are converging and at the same time flattens out after full time. This suggests that the cell is approaching its steady state in form of maximum achievable temperature under given conditions.



In Figure 16, the blue line and label are describing the mass-averaged temperature of the whole cell and the green line and label the stored energy in one double cell. After full time, the average temperature is 32,5°C which corresponds to 12,6 MJ stored energy in form of heat for a double cell. This is about 67 % of total capacity of the heat storage.

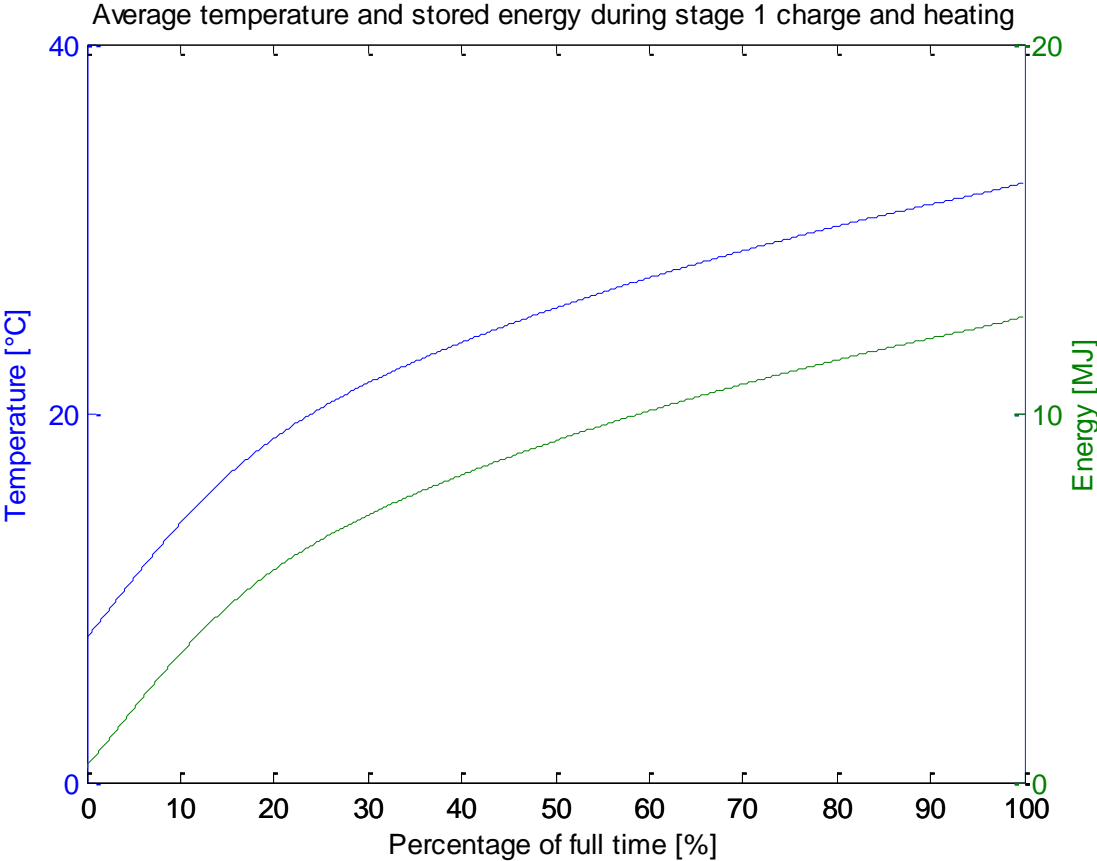


**Figure 16 Average temperature and stored energy**

#### 6.4.2.1 Contours after 3,3 % of full time

Figure 17 shows the temperature on the outer boundaries of the computational domain (left), the center plane normal to the x-direction (middle) and the center plane normal to the y-direction (right) after 3,3 % of full time of heating and stage 1 charging. The temperature in the top has already increased by around 8°C. The lower two is still at the starting temperature. The x-plane clearly shows how the heat from the pole bridge is transferred down through the plate package. Furthermore, the cooling of the plate edges by the electrolyte is clearly visible in the plane. From the y-plane plot it is obvious that the channels are the major heating source at this point in time. The effect of circulation, i.e. low temperatures at the upper part of the electrolyte, is depicted in the outer surface plot.

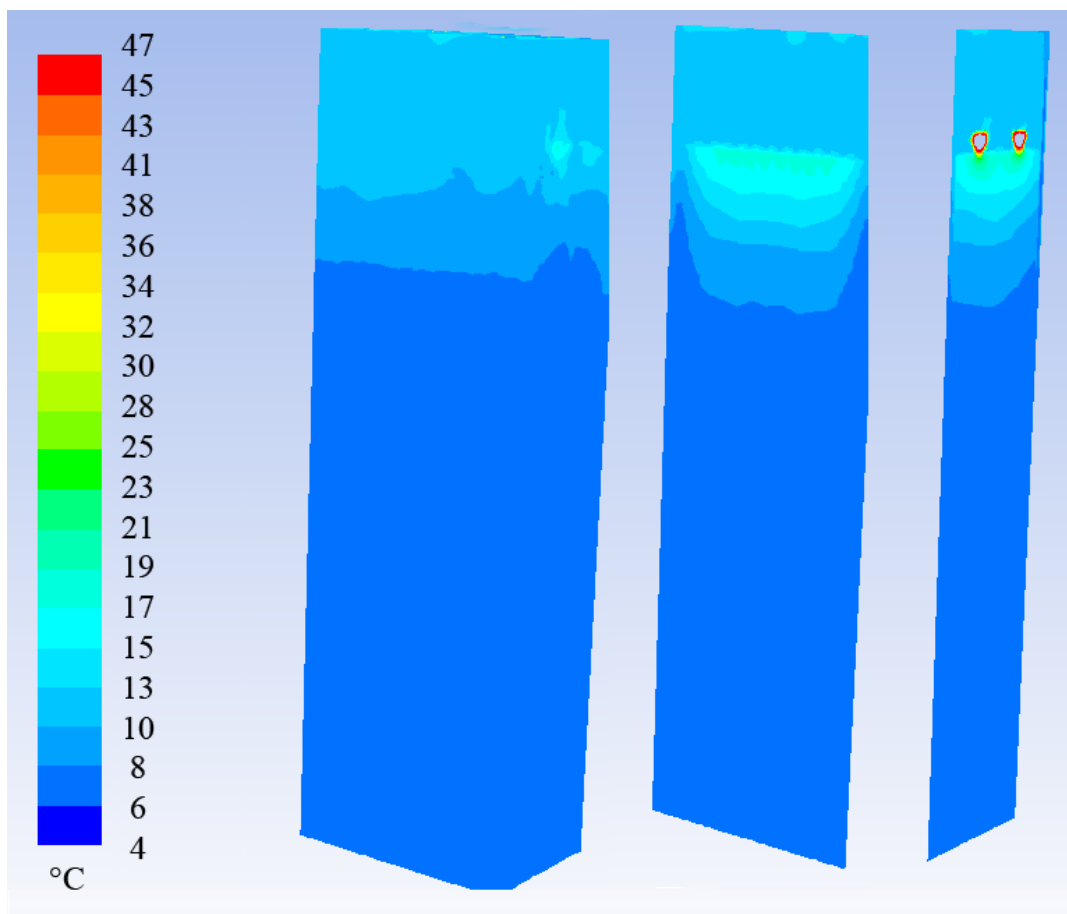
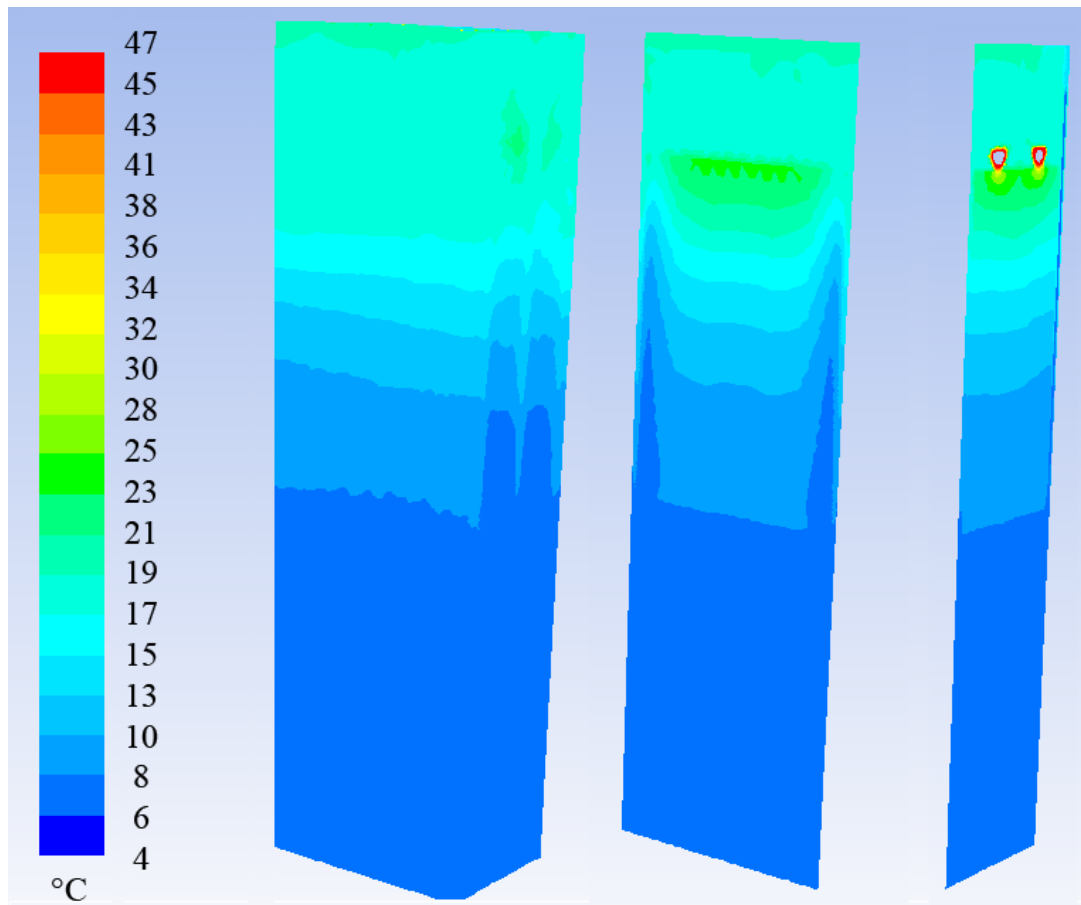


Figure 17 Temperatures after 3,3 % of full time of stage 1 charge and heating

#### 6.4.2.2 Contours after 10 % of full time

Figure 18 shows increasing differences between top and bottom temperatures and also that the vertical plates connected to the channels are not at this point helping to disperse the heat because they are not yet heated. The circulation does not seem to be good enough to disperse the temperatures more equally over the whole cell. The trend is the same as it was in Figure 17, but after 10 % of full time the whole upper plate package has increased in temperature making a clear line to the electrolyte in the middle. The temperature just under the channels is around 27°C. The electrolyte in the top has a temperature of about 17°C, but a small layer of electrolyte of a higher temperature has begun to settle just under the lid of the cell.



**Figure 18 Temperatures after 10 % of full time of heating and stage 1 charge**

### 6.4.2.3 Contours after 30 % of full time

After 30 % of full time the temperature differences between the top and bottom has reached its highest values which can be seen in Figure 19. The upper plate package has a higher temperature, and is increasing quicker, than the lower despite the internal heat generation is equal. This means that the heat transfer from the pole bridge is still having a large effect on the upper plate package and the direct heat transfer to the vertical plates is leading to an increased temperature, but still much lower than the surroundings. The temperature shows a continuous increase over the cell height, instead of clear stratification, observed at previous time instants. The electrolyte in the top has now reached a temperature of about 27°C, but the highest temperature is still in the connection between the pole bridge and the upper plate package. The temperature here is at this moment about 32°C, while the temperature in the lower plate package is about 14°C.

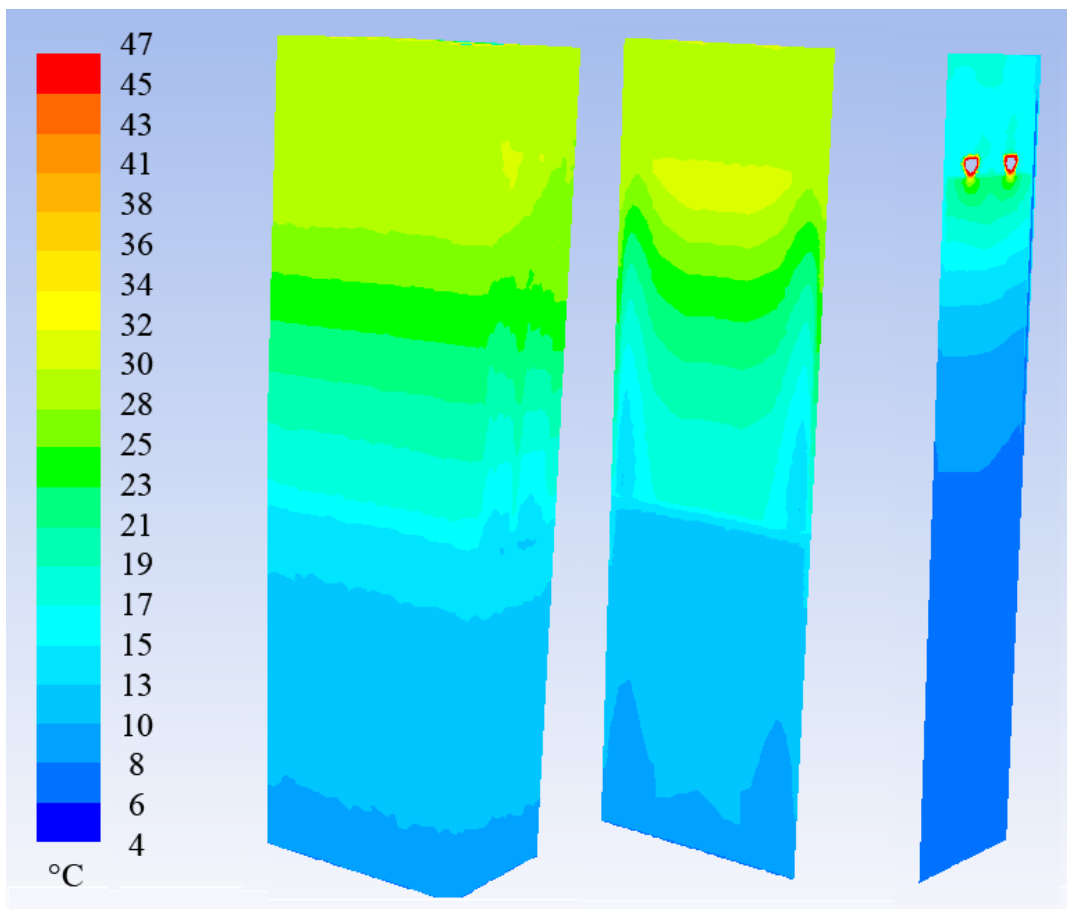


**Figure 19** Temperatures after 30 % of full time of heating and stage 1 charge

#### 6.4.2.4 Contours after 60 % of full time

Figure 20 shows one of the effects of the circulation, which is that a small portion of the electrolyte at the top of the cell is pushed down on the right side from the left point of view. The circulation pump can be seen in the view to the right, furthest to the right. The electrolyte just over the outlet from the circulation has a temperature of 24 degrees, which is about 8 degrees colder than the average temperature of the top electrolyte. The temperature rise can now be observed over the whole cell, but the lower plate package and the lower pole bridges have still got a relatively low temperature of about 17°C. The upper plate package has reached temperatures from 25 to 41°C.

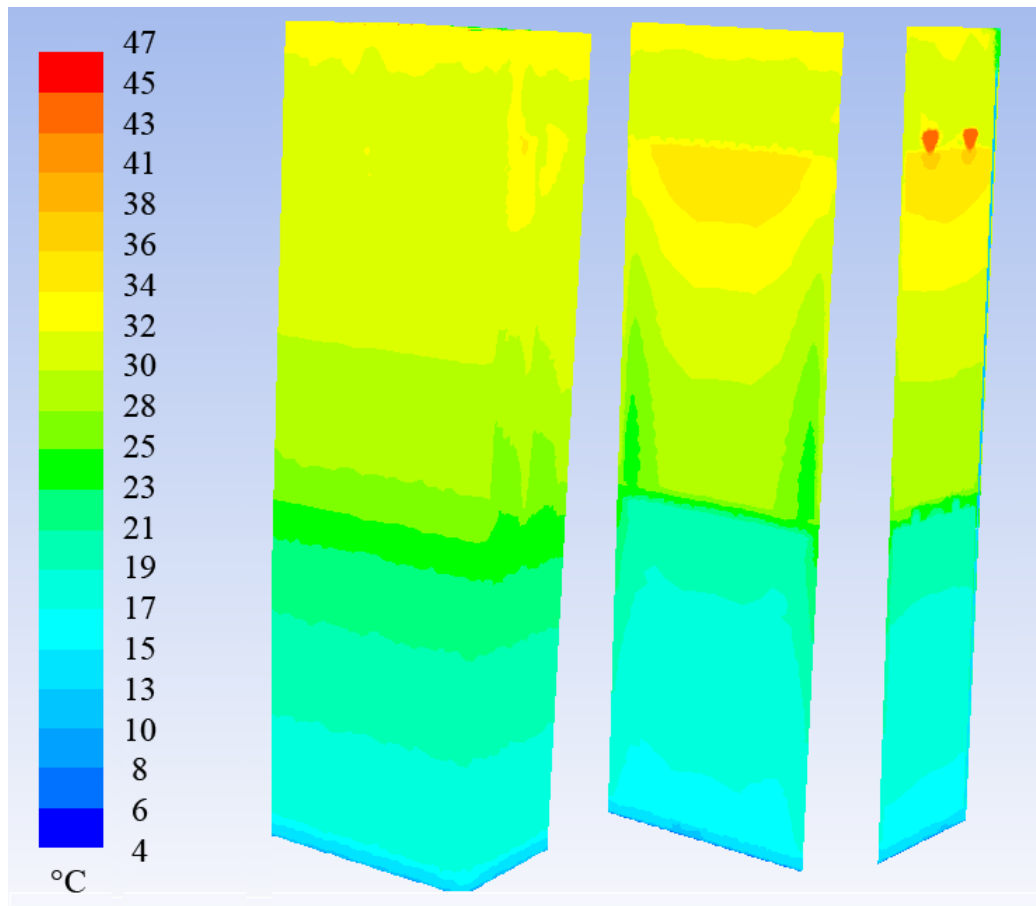
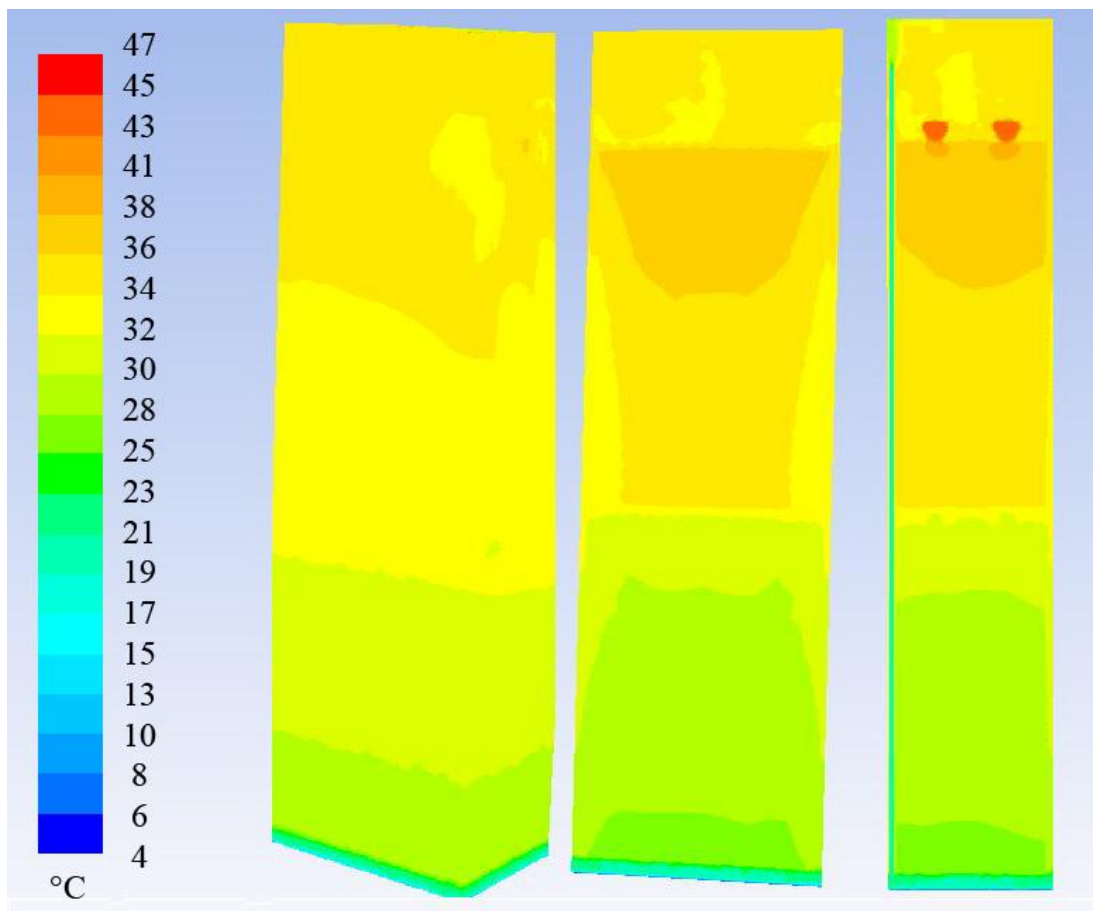


Figure 20 Temperatures after 60 % of full time of stage 1 charge and heating

#### 6.4.2.5 Contours after full time

After full time of heating and charging with stage 1 the cell temperatures are according to Figure 21. The majority of the electrolyte and the upper plate package have a temperature of 33-38°C, while the lower plate package is a few steps behind with temperatures of 25-29°C. The lower temperature fields in the top electrolyte are probably an effect from the forced circulation together with the natural circulation. The temperature in the top has already, more or less, reached its maximum value, while the temperatures further down in the cell are slowly increasing their temperatures and therefore reducing the difference to the top. Figure 21 illustrates the end state of the cell after stage 1 charge with internal heat generation. This state will also be the starting state of next case, where stage 2 charging is performed.



**Figure 21** Temperatures after full time of heating and stage 1 charge

## 6.5 Case 2: Heating combined with stage 2 charging

### 6.5.1 Conditions

- Heat generation in both plate packages of  $280\text{W/m}^3$ .
- Initial values are the results after full time of case 1.
- Duration of stage 2: 2h and 20 minutes

### 6.5.2 Results and comments

Figure 22 shows how the temperature varies over time during a stage 2 charge when the cell already has been heated from stage 1 charge and pole heating. Generally, the temperatures are not increasing by very much. Monitor point 4, in the lower plate package, has been increasing the most in temperature over the 2 hours and 20 minutes, which can be seen in Table 17.

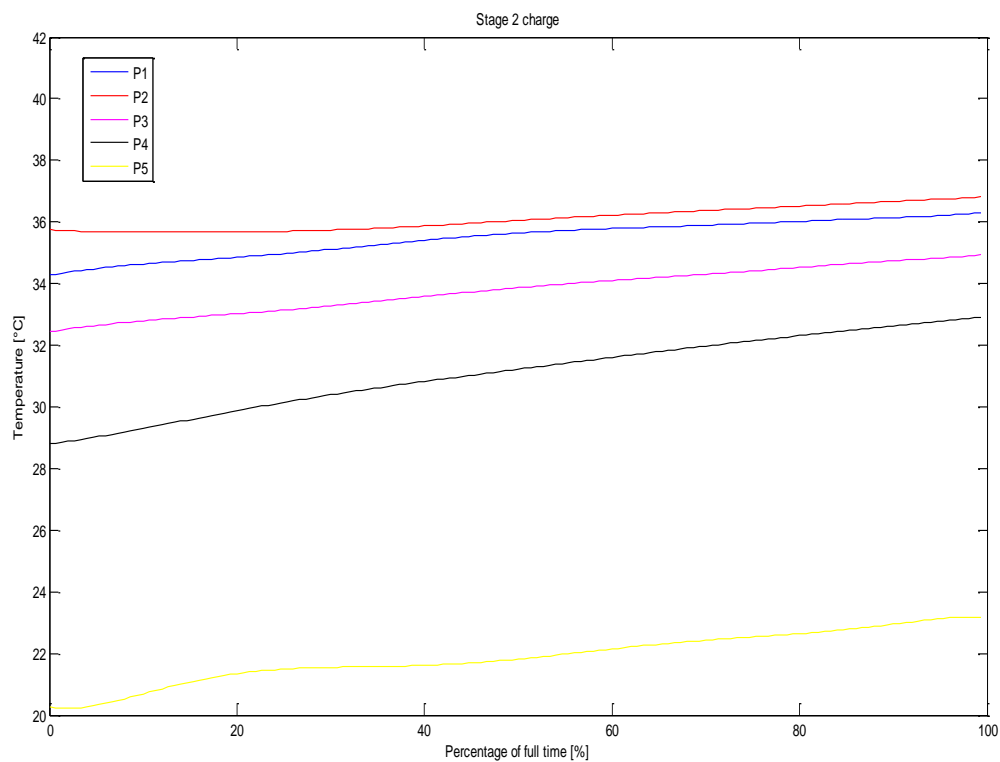


**Figure 22 Temperature versus time during stage 2 charge**

**Table 17 Increased temperature during stage 2 charge and heating**

	P1	P2	P3	P4	P5
$\Delta T$	2,1	2,1	2,5	4,2	3,7

Figure 23 shows how the mass averaged temperature and the stored heat are changed over the time for stage 2 charge and heating. After full time of stage 2 charge when the heating is turned off, the cell has stored 72 % of the heat storage potential. Since the average temperature gradient is very small, the cell is probably near its steady state which means that further heating is unnecessary due to the time versus increased temperature ratio.

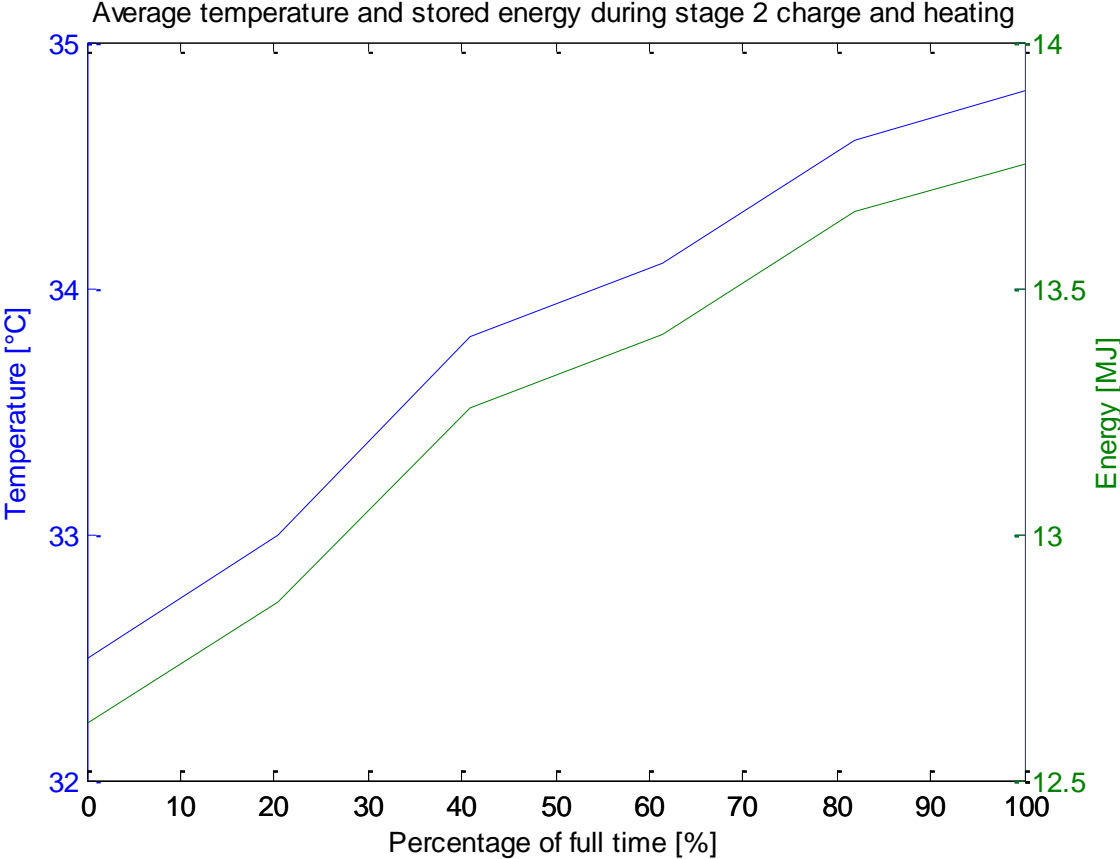


**Figure 23 Average temperature and stored energy during stage 2 charge and heating**



### 6.5.2.1 Contours after full time of stage 2 charge

The final state of the temperatures is showed in Figure 24. The figure shows that the temperatures are almost alike everywhere in the cell except in the bottom. This can also be seen in Figure 22 where monitor points 1-4 has a final difference of only 6 degrees.

The green line on the left in the view to the right is the circulation which is transferring 25 degeed electrolyte from the bottom to the top. The cell is probably very near its steady state because the gradients are very small and the temperature is almost homogenous in the whole cell.

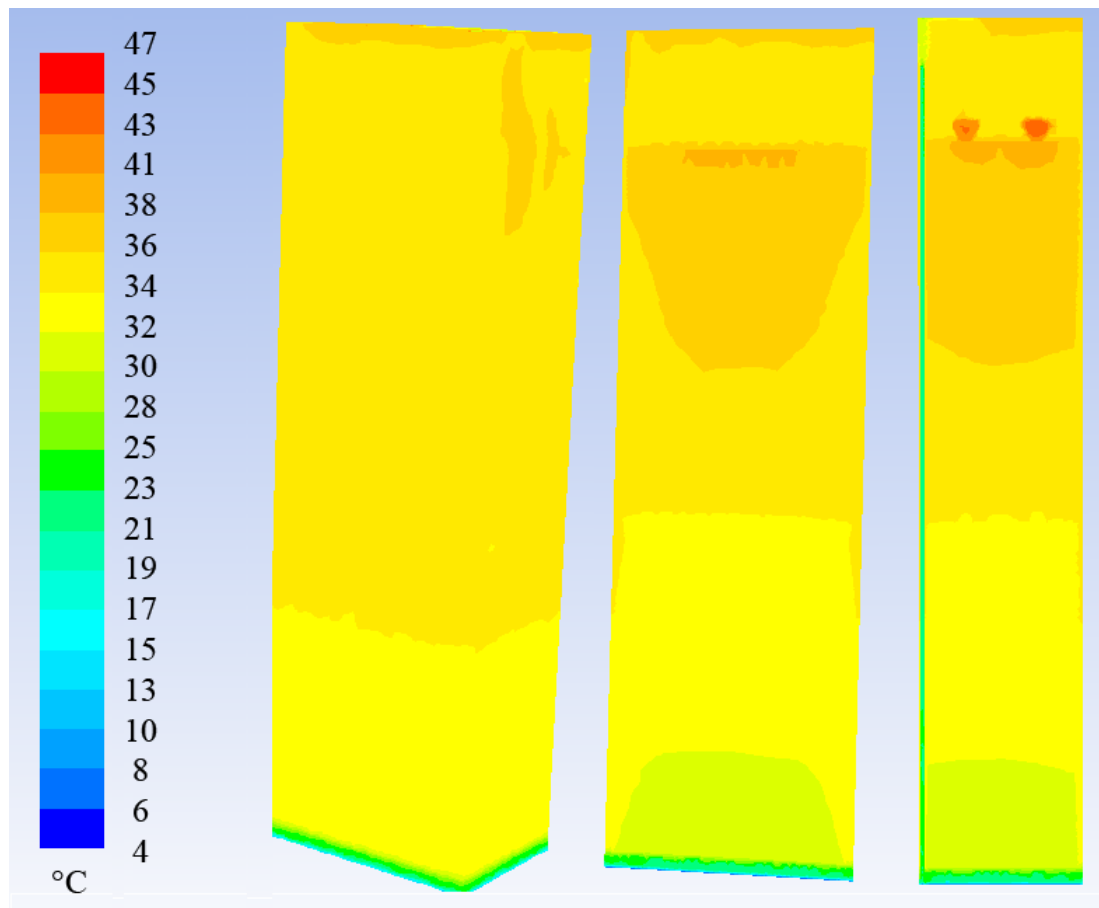


**Figure 24 Final temperatures after full time of heating**

## 7 Discussion and conclusions

It is clear that the diesel engines produces a large amount of waste heat, both through the exhaust gas and by the cooling of the engine block, which is with margin enough to use in the heating circuit for the batteries. The fact that the diesel engines are running so infrequently makes the time it takes for the batteries to absorb the heat the limiting factor.

The results clearly show how long time it takes for the cell to absorb the heat delivered through the pole bridge and the internal generation. The time it takes is much less than expected, suggesting a good quality of the heating/cooling system in the pole bolt and pole bridge. Already after case 1 with stage 1 charge combined with heating, the cell has absorbed enough energy to be useful not only for the performance of the batteries but also for the on-board comfort.

Periodically the difference of local temperatures inside the cell is pretty large. This is alarming since it is not known how this will affect the chemical processes that are executed during charging or the properties of the materials. This difference could be decreased by having a lower temperature in the water flow and, thus achieving the same temperature, however after a longer heating time. It is also possible to use intermittent heating, utilizing the circulation to equalize the acid temperature in the cell. Two reasons for the large differences of temperature are that the heating, except the internal generation, is just performed in the top of the cell and the circulation of the electrolyte is not good enough. If it would be possible to get the heating water to the lower pole bridges, the differences would be reduced and the time for heating would be less. This does not seem as impossible since the lower pole bridge already has the same shape with the channel inside, prepared to be used. The main difficulty with this is how to lead the water down to the bridge since there are very little of free space in the cell. One may solve this by adding a pipe, like the circulation pipe, between the plates, or by enlarging the vertical plates and mold a channel inside them. Today the vertical plates have a thickness of 11mm which is too thin to have a water flow inside.

It is also clear that the heating of the cells will under a relatively short time increase the capacity of the batteries significantly. Consideration has to be made that the heating system is a slow system which takes some time to heat up before it is able to transfer heat to the cell. In case 1 the starting temperature of the heating fluid is assumed to be at 45°C already when the process begins, which is not the case in reality. This means that the cell will be dormant for some time before starting to absorb the heat and the temperatures after 100 % of case 1 will be lower. At the same time, the water circuit will be warm for a while after the diesel engines have been shut down and will therefore compensate for the loss in time at startup. A further issue to consider is that higher temperatures generally shorten the life time of a battery.

The heating during stage 2 charge had less effect than predicted, and the increased temperature was small. This is probably because of a smaller temperature difference between the heating water and the cell, and also because of the smaller internal heat generation in a stage 2 charge. However, the time for stage 2 charge is valuable because the temperatures in the cell become more uniform which will counteract stratification.

It is clear, based on the results in this report, that the idea of storing heat in the batteries is possible during a reasonable time limit of heat transfer. My recommendations, to Kockums AB and FMV, is that this system will be useful and is worth further investigations which may be based on the CFD-files leaved behind from this diploma work.

## 8 Future work

During this Master Thesis a couple of questions have appeared, where some are needed to be investigated before any decision are taken and others are just ideas worth mentioning.

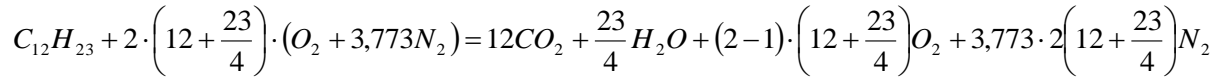
- For how long will the heat inside the batteries influence the climate on-board?  
A large part of the heat will probably disperse directly through the hull and out to the sea. A 2-D geometry including mesh is available to follow up and simulate where the heat will disappear and for how long useful heat is available.
- Calculate what time it will take to switch from heating the batteries to start cooling them if the operation profile changes and the temperature therefore reaches its critical limit.
- Is it possible to reduce the differences in temperature inside the cell?  
By having a lower temperature in the heating water and extending the time for heat transfer, the local temperatures will be more uniform. Another idea is to increase the circulation of the electrolyte or build a connection to the lower pole bridge making it possible to transfer heat further down in the cell.
- How will the higher temperature in the batteries affect the hydrogen formation?
- How to integrate the new system to the hot water circuit?
- Is it possible to use a heat pump to get better use of the heat?
- Instead of using the batteries as accumulators for heat, is it possible to change the lead that is used for ballast to a saline solution that will be much better to store and deliver heat?
- Generate more information from existing data-files  
The data-files from the simulations include a lot of other information that is not presented in this report. This information can be of interest in other calculations, it is for instance relatively easy to acquire the heat transferred in the pole bridge with decreasing  $\Delta T$ .

## References

1. **Ubåtskännedom.** *Internal document.* 2011.
2. **Handbok Huvudbatteri.** *Internal document: Handbok Huvudbatteri Ubåtar typ VGD/SÖD.*
3. **Battery stuff webpage.** [Online] [Cited: February 1, 2011.] [http://www.batterystuff.com/tutorial\\_battery.html](http://www.batterystuff.com/tutorial_battery.html).
4. General Scalar Transport Equation: Discretization and Solution. *ANSYS FLUENT 12.0 Theory Guide.* pp. 18-8.
5. The Octree Mesh Method, Robust (Octree). *Documentation for ANSYS ICEM CFD 12.0.*
6. **Eymard, R, Gallouët, T and Herbin, R.** *Finite Volume Methods.* 2003.
7. CFD-Wiki, the free CFD reference. [Online] [Cited: april 15, 2011.] [www.cfd-online.com/wiki/Finite\\_volume](http://www.cfd-online.com/wiki/Finite_volume).
8. Energy equations. *ANSYS FLUENT 12.0 Theory Guide.* p. Ch. 5.
9. Energy equation in Solid Region. *ANSYS FLUENT 12.0 Theory Guide.*
10. Transport equations for the Realizable k-e Model. *ANSYS FLUENT 12.0 Theory Guide.* pp. 4-20.
11. Solver Theory SIMPLE. *Ansys Theory Guide 12.0.*
12. **Johansson, Bengt.** Förbränningsmotorer. 2006, p. 149.
13. **Wester, Lars.** *Tabeller och diagram för energitekniska beräkningar.* 2009.
14. *Internal document: Drawing nr: A19-9D411-1HTM.*
15. **Cooling Main Battery NOLI, Enclosure 8.** *Internal document; Enersys infomation.*
16. **Energirådgivningen.** *Energirådgivningen.* [Online] [Cited: Mars 10, 2011.] [http://www.energiradgivningen.se/index.php?option=com\\_content&task=view&id=70&Itemid=1](http://www.energiradgivningen.se/index.php?option=com_content&task=view&id=70&Itemid=1).
17. Internal documentation from supplier.
18. **Engineering toolbox.** *Engineering Toolbox.* [Online] [Cited: February 20, 2011.] [http://www.engineeringtoolbox.com/air-properties-d\\_156.html](http://www.engineeringtoolbox.com/air-properties-d_156.html).
19. Matbase. [Online] [Cited: February 20, 2011.] [www.matbase.com/material](http://www.matbase.com/material).
20. **Sundén, Bengt.** [interv.] Henrik Hed. 2010.
21. **Sundén, Bengt.** *Värmeöverföring.* s.l. : Studentlitteratur, 2006. ISBN 91-44-00087-1.
22. **Photo cell.** *Internal picture "supplier 037.jpg" in folder "Foto supplier", owner Tor Göransson.*
23. **Bengtsson, Per.** *KAB.*
24. *Internal documentation: Batteriinstallationer Ubåt typ GTD.*
25. Diesel Fuel. *Wikipedia.* [Online] [Cited: February 25, 2011.] [www.wikipedia.org/wiki/Diesel\\_fuel](http://www.wikipedia.org/wiki/Diesel_fuel).

# Appendix A: Complete calculations

## A1. Available heat in the exhaust gases



$$x_{H_2O} = \frac{n_{H_2O}}{n} = \frac{5,75}{12 + 5,75 + 17,75 + 133,942} = 0,0339$$

$$x_{CO_2} = \frac{n_{CO_2}}{n} = \frac{12}{12 + 5,75 + 17,75 + 133,942} = 0,0708$$

$$\frac{x_{H_2O}}{x_{CO_2}} = 0,4792$$

$$x_{CO_2}$$

The result, together with exhaust temperature of 550°C, will be used in **Chart 1** to determine the specific heat of the exhaust gas to  $cp_{exhaust} = 1,47kJ/kg$

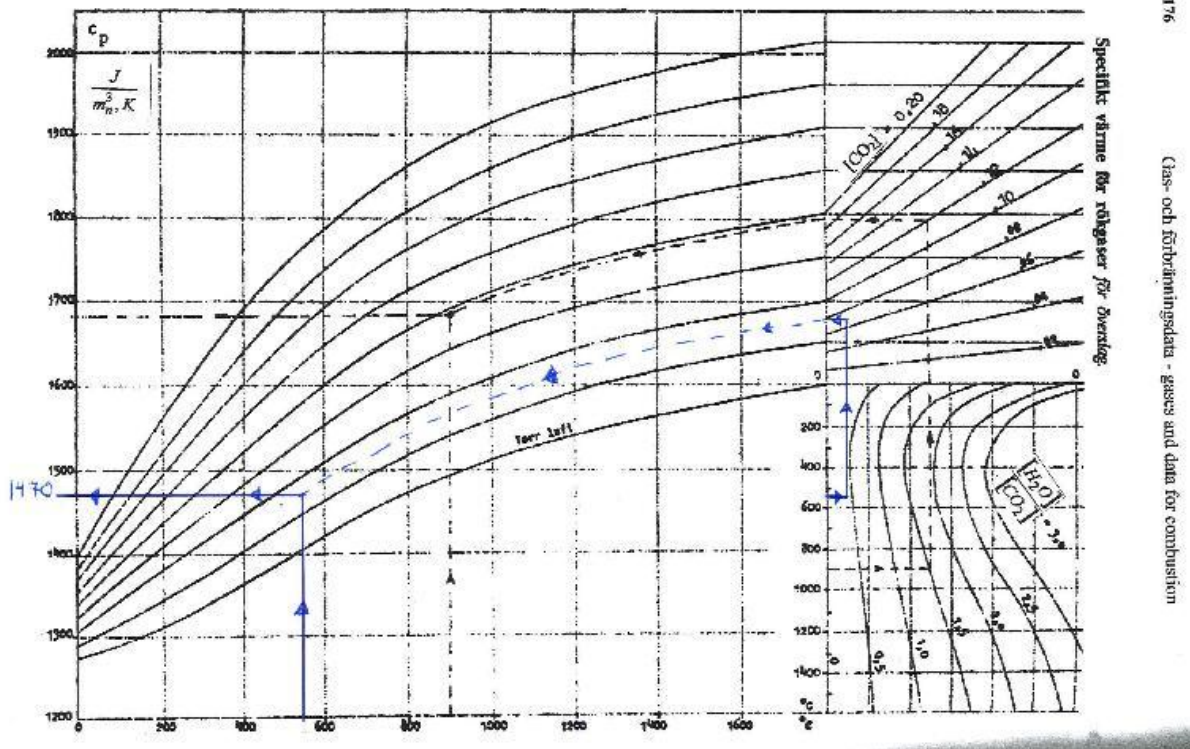


Chart 1 [13]

$$\dot{m} = 2,351kg/s$$

$$T_1 = 550^\circ C$$

$$T_2 = 250^\circ C$$

$$cp = 1,47kJ/kgK$$

$$Q = \dot{m} \cdot cp \cdot (T_1 - T_2) = 1037kW$$

With both engines running this gives available heat of

$$Q_{tot} = 2 \cdot 1037 = 2074kW$$

## A2. Potential heat storage in the batteries

Substance	Mass(kg)	C <sub>p</sub> (kJ/(kgK))
Lead(Pb)	272,5	0,13
Copper(Cu)	52,5	0,39
Sulphuric acid(H <sub>2</sub> SO <sub>4</sub> )	49	1,38
Water(H <sub>2</sub> O)	74,5	4,18
Other materials	36,5	1,6
Total/Average	485	1,02

$$T_1 = 7^\circ C$$

$$T_2 = 45^\circ C$$

$$c_{p,avg} = (\sum m_i \cdot c_{p_i}) / m_{total}$$

$$c_{p,avg} = \frac{(272,5 \cdot 0,13 + 52,5 \cdot 0,39 + 49 \cdot 1,38 + 74,5 \cdot 4,18 + 36,5 \cdot 1,6)}{(485)} \approx 1,02 \text{ kJ}/(\text{kgK})$$

$$Q_{cell} = m \cdot c_{p,avg} \cdot \Delta T$$

$$Q = 485 \cdot 1,02 \cdot (45 - 7) = 18,799 \text{ MJ}$$

## A3. Acid outside the plate package

The following calculation is based on distances according to drawing of the cell and the CAD model. The free volume is the volume that doesn't include the electrolyte in between the plates.

$$\text{On top: } V_1 = 5,76 \text{ dm}^3$$

$$\text{In middle: } V_2 = 1,31 \text{ dm}^3$$

$$\text{In bottom: } V_3 = 0,87 \text{ dm}^3$$

$$\text{Along the sides: } V_4 = 0,75 \text{ dm}^3$$

$$\text{Total: } V_{free} = 8,7 \text{ dm}^3$$

$$m_{free} = V_{free} \cdot \rho_{acid} = 8,7 \cdot 1,3 = 11,31 \text{ kg}$$

$$m_{plate-acid} = m_{total} - m_{free} = 2 \cdot 19 \cdot 1,3 - 11,31 = 38,1$$

#### A4. Specific heat capacity for the plate package

$\mu$  is the fraction of the mass for a certain material.

The given data is

$$cp_{pb} = 0,128kJ/(kgK)$$

$$cp_{Cu} = 0,39kJ/(kgK)$$

$$cp_{plastic} = 1,6kJ/(kgK)$$

$$cp_{H_2SO_4} = 1,38kJ/(kgK)$$

$$cp_{H_2O} = 4,18kJ/(kgK)$$

The acid is a mixture of 39,5 mass-% sulphuric acid and 60,5 mass-% water.

$$cp_{acid} = 0,395 \cdot 1,38 + 0,605 \cdot 4,18 = 3,074kJ/(kgK)$$

The mass of the different materials are

$$m_{pb} = 96,76kg$$

$$m_{Cu} = 13,62kg$$

$$m_{plastic} = 1kg$$

$$m_{acid} = 38,1kg$$

$$m_{total} = 149,48kg$$

which gives a mass fraction rate of

$$\mu_{pb} = \frac{96,76}{149,48} = 0,647$$

$$\mu_{Cu} = \frac{13,62}{149,48} = 0,0911$$

$$\mu_{plastic} = \frac{1}{149,48} = 0,0067$$

$$\mu_{acid} = \frac{38,1}{149,48} = 0,255$$

for each material.

The average specific heat will be

$$cp_{avg} = 0,128 \cdot 0,647 + 0,39 \cdot 0,0911 + 0,0067 \cdot 1,6 + 0,255 \cdot 3,074 = 0,913kJ/(kgK)$$

#### A5. Average density for the plate package

To total mass and volume is known in the plate package. The total volume is

$V_{package} = 0,01104m^3$ . This will give us the following density

$$m_{package} = \frac{m_{total}}{4} = \frac{149,48}{4} = 37,4kg$$

$$\rho_{avg} = \frac{m_{package}}{V_{package}} = \frac{37,4}{0,01104} = 3385,7kg/m^3$$

### A6. Total thermal conductivity for the plate package

$$\delta_{group} = 3,44mm$$

$$\delta_{pb} = (25 + 7,5) \cdot 0,06554 = 2,13mm$$

$$\delta_{Cu} = 7,5 \cdot 0,06554 = 0,49mm$$

$$\delta_{plastic} = 1 \cdot 0,06554 = 0,066mm$$

$$\delta_{acid} = 9 \cdot 0,06554 = 0,59mm$$

	Lead(Pb)	Copper(Cu)	Plastic	Sulphuric acid(H <sub>2</sub> SO <sub>4</sub> )
C <sub>p</sub> [kJ/(kgK)]	0,128	0,39	1,6	1,38
λ [W/(mK)]	35,2	398	0,23	0,26
m [kg]	96,8	13,6	1	49,4(total)
ρ [kg/m <sup>3</sup> ]	11200	8950	1410	1300

	Thickness (δ) [mm]
Lead(Pb)	2,13
Copper(Cu)	0,49
Separators(plastic)	0,066
Electrolyte	0,59
<b>1 group</b>	<b>3,44</b>

**Y:**

$$\frac{\delta_{total}}{\lambda_{total} \cdot A} = \sum \frac{\delta_i}{\lambda_i \cdot A_i}$$

$$\frac{0,08256}{\lambda_y \cdot A} = \frac{24}{A \cdot 1000} \cdot \left( \frac{2,13}{35,2} + \frac{0,49}{398} + \frac{0,066}{0,23} + \frac{0,59}{0,26} \right)$$

$$\lambda_y = 1,31W/(mK)$$

**X :**

$$b_x = 0,0786m$$

$$N = 24st$$

$$L_x = 0,117m$$

$$A_{pb,x} = \delta_{pb} \cdot L_x = 0,000249m^2$$

$$A_{Cu,x} = \delta_{Cu} \cdot L_x = 0,000057m^2$$

$$A_{plastic,x} = \delta_{plastic} \cdot L_x = 0,0000077m^2$$

$$A_{acid,x} = \delta_{acid} \cdot L_x = 0,000069m^2$$

$$A_x = N \cdot \sum A_i = 0,00919m^2$$



$$R_{Pb,X} = \frac{b_X}{\lambda_{Pb} \cdot A_{Pb,X}} = 8,97K/W$$

$$R_{Cu,X} = \frac{b_X}{\lambda_{Cu} \cdot A_{Cu,X}} = 3,46K/W$$

$$R_{Plastic,X} = \frac{b_X}{\lambda_{Plastic} \cdot A_{Plastic,X}} = 44381,2K/W$$

$$R_{acid,X} = \frac{b_X}{\lambda_{acid} \cdot A_{acid,X}} = 4381,3K/W$$

$$R_X = \frac{1}{N \cdot \left( \frac{1}{R_{Pb,X}} + \frac{1}{R_{Cu,X}} + \frac{1}{R_{Plastic,X}} + \frac{1}{R_{acid,X}} \right)} = 0,104K/W$$

$$\lambda_X = \frac{b_X}{A_X \cdot R_X} = 82,3W/(mK)$$

Z :

$$b_Z = 0,117m$$

$$N = 24st$$

$$L_Z = 0,048m$$

$$A_{Pb,Z} = \delta_{Pb} \cdot L_Z = 0,002555m^2$$

$$A_{Cu,Z} = \delta_{Cu} \cdot L_Z = 2,35^{-5}m^2$$

$$A_{plastic,Z} = \delta_{plastic} \cdot L_Z = 3,17 \cdot 10^{-6}m^2$$

$$A_{acid,Z} = \delta_{acid} \cdot L_Z = 2,832 \cdot 10^{-5}m^2$$

$$A_Z = N \cdot \sum A_i = 0,06264m^2$$

$$R_{Pb,Z} = \frac{b_Z}{\lambda_{Pb} \cdot A_{Pb,Z}} = 1,3K/W$$

$$R_{Cu,Z} = \frac{b_Z}{\lambda_{Cu} \cdot A_{Cu,Z}} = 12,5K/W$$

$$R_{Plastic,Z} = \frac{b_Z}{\lambda_{plastic} \cdot A_{Plastic,Z}} = 160471,8K/W$$

$$R_{acid,Z} = \frac{b_Z}{\lambda_{acid} \cdot A_{acid,Z}} = 15889,8K/W$$

$$R_Z = \frac{1}{N \cdot \left( \frac{1}{R_{Pb,Z}} + \frac{1}{R_{Cu,Z}} + \frac{1}{R_{Plastic,Z}} + \frac{1}{R_{acid,Z}} \right)} = 0,0491K/W$$

$$\lambda_Z = \frac{b_Z}{A_Z \cdot R_Z} = 38,07W/(mK)$$

## A7. Thermal conductivity and specific heat capacity for the lower pole bridges

The total thermal conductivity is

$$\frac{0,0307}{\lambda \cdot A} = \frac{1}{A} \left( \frac{2 \cdot 0,005}{35,2} + \frac{2 \cdot 0,003}{398} + \frac{0,0147}{0,0257} \right)$$

$$\lambda = 0,0536447 \text{ W / (mK)}$$

The volumes and masses are

$$V_{pb} = 1,93 \cdot 10^{-4} \text{ m}^3$$

$$m_{pb} = 2,162 \text{ kg}$$

$$V_{Cu} = 9,17 \cdot 10^{-5} \text{ m}^3$$

$$m_{Cu} = 0,82 \text{ kg}$$

$$V_{air} = 1,30 \cdot 10^{-4} \text{ m}^3$$

$$m_{air} = 1,57 \cdot 10^{-4} \text{ kg}$$

$$V_{total} = 4,147 \cdot 10^{-4} \text{ m}^3$$

$$m_{total} = 2,98 \text{ kg}$$

The total density is

$$\rho_{total} = \frac{m_{total}}{V_{total}} = 7186 \text{ kg / m}^3$$

The specific heat is

$$cp_{total} = \sum \mu_{mass} \cdot cp_i = \frac{2,162}{2,98} \cdot 0,128 + \frac{0,82}{2,98} \cdot 0,39 + \frac{1,57 \cdot 10^{-4}}{2,98} \cdot 1,005 = 0,200 \text{ kJ / (kgK)}$$

### A8. Thermal conductivity for the vertical plates connecting the pole bridges

The material properties are calculated in analogy with the equations for the plate packages. The thickness and area of the materials are

$$\delta_{pb} = 2 \cdot 3 = 6mm$$

$$\delta_{Cu} = 5mm$$

X :

$$b_x = 0,085m$$

$$N = 1st$$

$$L_x = 0,6555m$$

$$A_{pb,x} = \delta_{pb} \cdot L_x = 0,0019665m^2$$

$$A_{Cu,x} = \delta_{Cu} \cdot L_x = 0,0032775m^2$$

$$A_x = 2 \cdot A_{pb,x} + A_{Cu,x} = 0,005244m^2$$

$$R_{pb,x} = \frac{b_x}{\lambda_{pb} \cdot A_{pb,x}} = 1,22795K/W$$

$$R_{Cu,x} = \frac{b_x}{\lambda_{Cu} \cdot A_{Cu,x}} = 0,065162K/W$$

$$R_x = \frac{1}{\left( \frac{1}{R_{pb,x}} + \frac{1}{R_{Cu,x}} + \frac{1}{R_{pb,x}} \right)} = 0,05891K/W$$

$$\lambda_x = \frac{b_x}{A_x \cdot R_x} = 275,15W/(mK)$$

The thermal conductivity in the Y-direction is

$$\frac{0,006 + 0,005}{\lambda \cdot A} = \frac{1}{A} \left( \frac{2 \cdot 0,003}{35,2} + \frac{0,005}{398} \right)$$

$$\lambda_y = 60,1W/(mK)$$

Z :

$$b_Z = 0,6555m$$

$$N = 1st$$

$$L_Z = 0,085m$$

$$A_{Pb,Z} = \delta_{Pb} \cdot L_Z = 2,55 \cdot 10^{-4} m^2$$

$$A_{Cu,Z} = \delta_{Cu} \cdot L_Z = 4,25 \cdot 10^{-4} m^2$$

$$A_Z = 2 \cdot A_{Pb,Z} + A_{Cu,Z} = 9,35 \cdot 10^{-4} m^2$$

$$R_{Pb,Z} = \frac{b_Z}{\lambda_{Pb} \cdot A_{Pb,Z}} = 73,028K / W$$

$$R_{Cu,Z} = \frac{b_Z}{\lambda_{Cu} \cdot A_{Cu,Z}} = 3,873K / W$$

$$R_Z = \frac{1}{\left( \frac{1}{R_{Pb,Z}} + \frac{1}{R_{Cu,Z}} + \frac{1}{R_{Pb,Z}} \right)} = 3,5034K / W$$

$$\lambda_Z = \frac{b_Z}{A_Z \cdot R_Z} = 200,1W / (mK)$$

#### A9. Specific heat capacity for the vertical plates connecting the pole bridges

The density is

$$V_{Cu} = 2,58923 \cdot 10^{-4} m^3$$

$$V_{Pb} = 3,1071 \cdot 10^{-4} m^3$$

$$V_{tot} = V_{Cu} + V_{Pb} = 5,6963 \cdot 10^{-4} m^3$$

$$\mu_V = \frac{V_{Cu}}{V_{tot}} = 0,455$$

$$\rho_{vertical} = \mu \cdot \rho_{Cu} + (1 - \mu) \cdot \rho_{Pb} = 10176,25kg / m^3$$

The specific heat is

$$m_{Pb} = \rho_{Pb} \cdot V_{Pb} = 3,47995kg$$

$$m_{Cu} = \rho_{Cu} \cdot V_{Cu} = 2,317kg$$

$$m_{tot} = m_{Pb} + m_{Cu} = 5,7973kg$$

$$\mu_m = \frac{m_{Pb}}{m_{tot}} = 0,600$$

$$cp_{vertical} = \mu_m \cdot cp_{Pb} + (1 - \mu_m) \cdot cp_{Cu} = 0,2339kJ / (kgK)$$

	<u>Stage 1 charge</u>	<u>Stage 2 charge</u>
P[W/cell]	190	67,84
U[V]	0,47	0,47
I[A]	405,2	144.34
Previous discharge[Ah]		
V[m <sup>3</sup> ]	0.108	0,108
$\rho$ [kg/m <sup>3</sup> ]	1,19	1,285
dQ[W/cell]	182	30,1
Heat generation[W/m <sup>3</sup> ]	1693	280

### **A10. Internal heat generation**

$$dQ = I \cdot dU \cdot dt$$

$$dU = U - U_0$$

where  $U_0$  is the internal voltage.

The plate packages which will generate the internal heat has a volume of

$$V = 0,1075248m^3$$

#### Stage 1 charge:

*Given:*

$$P = 190W$$

$$U_{avg} = 0,47V$$

$t =$

The voltage is an average value that happens to be the same as the constant voltage of the step 2 charge. The density is taken from the table of density versus previous discharge which in this case is X Ah.

*Solution:*

$$I = \frac{P}{U} = 405,2A$$

$$\rho_{medel} = 1,19$$

$$U_0 = 0,02$$

$$dQ = 405,2 \cdot (0,47 - 0,02) = 182W / cell$$

$$\frac{P}{V} = \frac{182}{0,1075248} = 1693W / m^3$$

## Stage 2 charge

Given:

$$I = 280 \rightarrow 60A$$

$$t = 2,3h$$

$$U = 0,47V$$

The voltage will be of half value every hour and the current is constant. The previous discharge is assumed to be the discharge capacity before step 1 minus the capacity of step 1.

Solution:

$$280 \rightarrow 140A:$$

$$I_1 = \frac{280 + 140}{2} = 210A$$

$$t = 1h, \quad \mu_1 = \frac{1}{2,3} = 0,43$$

$$140 \rightarrow 70A:$$

$$I_2 = \frac{140 + 70}{2} = 105A$$

$$t = 1h, \quad \mu_2 = \frac{1}{2,3} = 0,43$$

$$70 \rightarrow 60A:$$

$$I_3 = \frac{70 + 60}{2} = 65A$$

$$t = 0,3h, \quad \mu_3 = \frac{0,3}{2,3} = 0,13$$

$$I_m = \sum \mu_i \cdot I_i = 144A$$

$$P_{cell} = U \cdot I_m = 67,6W$$

$$\rho = 1,285$$

$$U_0 = 0,025$$

$$dQ = 67,6 \cdot (0,47 - 0,025) = 30,1W / cell$$

$$\frac{P}{V} = \frac{30,1}{0,1075248} = 280W / m^3$$

$\mu_i$  is the time fraction of the different currents.

